

Bachelor Thesis Statement: Triantafyllaki Aikaterini-Niovi, ph4283  
University of Crete, Physics Department  
Supervisor: Pablo Reig



**Determination of the rotational velocity and spectral classification of  
four Be/X-ray binaries**

# Table of Contents

Acknowledgements.....	3
Abstract.....	4
1.Introduction.....	5
X-ray Binaries.....	5
Accretion in binary systems.....	7
2.Methodology.....	10
i. Reduction of Stellar Spectra.....	10
ii. Spectral Classification.....	11
iii.Rotational Velocity.....	12
3.Results.....	13
i.Spectral Class.....	13
ii. Rotational velocity.....	18
4.Discussion.....	29
Issues due to strong emission.....	29
Spectral Class.....	29
Rotational Velocities.....	30
5. Conclusion.....	34
6.Appendix.....	35
Python Script 1- putting all data under chi test and finding the best value.....	35
Python Script 2- binning procedure to fix the continuum.....	37
Fourier Transform.....	38
Reduction of Stellar Spectra with IRAF.....	39
7.References:.....	45

## **Acknowledgements**

I would like to take this opportunity to express my gratitude towards my thesis supervisor, Dr. Pablo Reig, for giving me the opportunity to work with him, for being patient with me, while I was learning all about the research process from the very early stages and , for his enthusiasm, every time I learnt something new, his willingness to answer all of my questions, his trust that I could fulfill my work within the time and freedom he gave me and last but not least, for his support and guidance throughout the past year. Thank you.

Additionally, I owe a very special thanks to Angelos Karakonstantakis for his kind support throughout the entire process. His friendship through the entire year and support that I can do everything, along the knowledge on Python and his contribution every time I failed to successfully write or run a code, were invaluable and I would not have been capable of learning all the new things required for this thesis statement and the research done -such as how to code using Python and how to use other software without him.

## **Abstract**

Be stars are very rapidly rotating B stars of the main sequence that, for a yet unknown reason, form an outwardly diffusing, gaseous Keplerian disk around their equator. The formation of this circumstellar disk is linked with mass ejection processes and fast rotation rates at the Be star's photosphere. This material has huge amounts of angular momentum and settles in an orbit around the star.

This work takes a closer look on four high mass X-ray binary whose accreting material is believed to come from their circumstellar disk. The systems that are analysed in this work are: IGR J01363+6610, IGR J01583+6713, SAX2239.3+6116, and KS 1947+300+300. The main objective of this work is to determine their spectral type and rotational velocities.

# 1.Introduction

## X-ray Binaries

X-ray binaries are systems which consist of a compact object orbiting a normal star - a star whose main mechanism for the production of energy is still hydrogen burning into helium through thermonuclear reactions. The compact companion can either be a black hole, a neutron star or a white dwarf. In X-ray binaries, there is a transfer of mass from the optical companion into the compact object by a mechanism known as accretion. The word “accretion” refers to any gradual accumulation or deposition of diffused gas or matter onto some object under the influence of gravity. The in-falling material spirals towards the accretor, and if it has enough angular momentum an accretion disc will form. In the case of a neutron star or a black hole, the matter falls down onto an enormous well of gravitational potential and is accelerated to extremely high velocities. <sup>[11,12]</sup>.

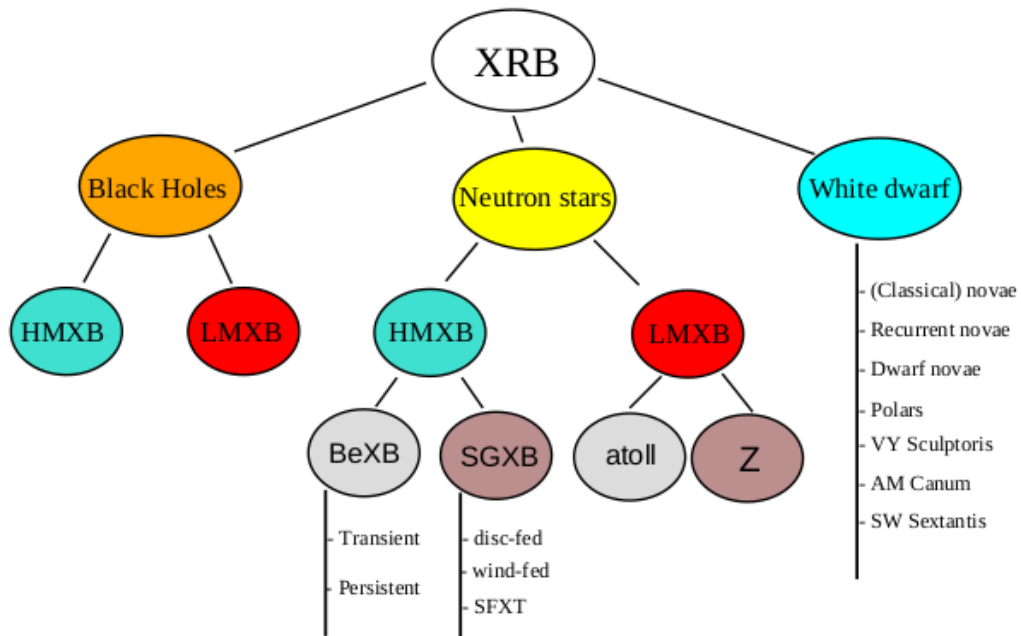


Image 1: Be/X-ray binaries classification, Reig P. 2011

A neutron star is the collapsed core of a giant star which, before collapsing, it had a total mass of between 10 and 29 solar masses. Neutron stars are the smallest and densest stars, not counting black holes. They have a radius on the order of 10 kilometres and a mass lower than 2.16 solar masses. They result from the supernova explosion of a massive star, along with gravitational collapse, that compresses the core past white dwarf star density to that of atomic nuclei<sup>[13]</sup>.

All the material gathered on or near the surface of the neutron star and the kinetic energy produced in free fall is then radiated as heat which results in making the system an X-ray source. The velocity of the matter during this free fall and when this kinetic energy is radiated away, are around half of the velocity of light.

According to the spectral type of the star donor, X-ray binaries can be divided into high mass (HMXB) and low mass X-ray binaries (LMXB). The spectral type is what will determine how the transfer of the material will happen.

In LMXB, the donor spectral type is later than type A and has a mass smaller than two solar masses and mass transfer occurs via Roche lobe overflow. The HMXBs contain a type O or B companion with high luminosity and they have  $M > 10$  solar masses. HMXBs are further divided into two groups, according to the with luminosity class I-II companion stars and Be/X-ray binaries with luminosity class III-V companions stars (BeXB).<sup>[11]</sup> In HMXBs, mass transfer occur via the strong stellar wind in SXR or from the circumstellar disk in BeXB..

Be/X-ray stars binary systems have a neutron star orbiting a O9e-B2e star. The system has a Be-type star that is spinning at very high speeds which sometimes makes the star to throw its own matter off into space. Be stars are fast-rotating B-type and luminosity class III-V stars which at some point in their lives, have shown spectral lines in emission. When a neutron star is in orbit around the Be star, some of the expelled matter will fall towards it and then accretion takes place and sometimes an accretion disk is formed. The orbits of these systems are often elliptical, meaning that at some points in their orbit the stars are closer together (resulting in a higher accretion rate and an extra spurt of X-ray emission) and at others they are further apart (causing a dip in the X-ray emission).

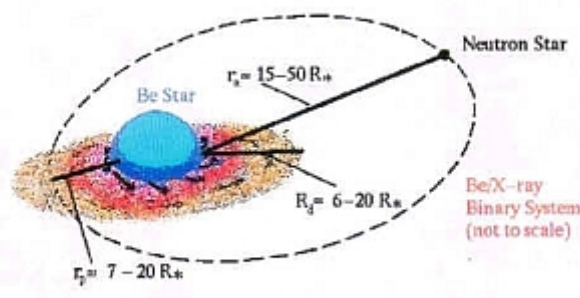


*Image 2: A Be/X Binary System not on scale.  
Image source: Skinakas Observatory*

In the Be stars the letter "e" stands for emission, as instead of the normal photospheric absorption lines, the optical spectra of Be stars display emission lines. Strong infrared emission and polarized light are another two defining characteristic of Be stars. The origin of these three observational properties (emission lines, infrared excess, and optical polarization) resides in a gaseous, equatorially concentrated circumstellar disc around the OB star. This disc constitutes the main source of variability in BeX. The matter transferred from the disc to the neutron star is responsible for the emission of high-energy radiation as a result of accretion. Thus, X-rays give information

about the physical conditions in the vicinity of the compact object, while optical/IR observations provide information about the massive companion. [11] Here it is important to clarify that these systems can have two types of disk. The circumstellar disk, also known as decretion disk around the Be star's equator and an accretion disk around the neutron star.

## **Accretion in binary systems**

### **The Roche Lobe.- The formation of an accretion disk**

In a binary star system, each star is exerting a gravitational force on any object with mass within its vicinity. A region can be defined inside of which the gravitational force from star 1 is stronger than star 2 and vice versa. The volume of space inside of which matter feels a stronger pull from star 1 than star 2 defines the Roche Lobe for star 1, and the volume of space, inside of which, matter feels a stronger pull from star 2 than star 1 defines the Roche Lobe for star 2. Any matter inside the Roche Lobe of an object will be gravitationally bound to that object. The two Roche Lobes, for the stars consisting a binary system are approximately teardrop shaped, and these shapes meet at the Lagrangian points. In celestial mechanics, the Lagrangian points are the points near two large bodies in orbit where a smaller object will maintain its position relative to the large orbiting bodies. There are five Lagrangian points in total, three of which are the most important ones. The two lobes of the star meet at a point known as L1, the first Lagrangian point or the inner Lagrangian point is where the gravitational spheres of influence of the two stars are connected. At L1 point, the gravitational force from both stars is exactly equal, so matter can actually go from being bound to one star into being bound to the other by passing through the L1 point. This means that, if one star starts to fill its Roche lobe (the part of the critical potential engulfing the star), then matter can flow through the L1 point into the Roche lobe of the other star.[15] . The overflow will occur at the point that the gravity of the two stars cancels and the material will fall from the Roche Lobe of the Giant Star to the neutron star, forming an accretion disk.

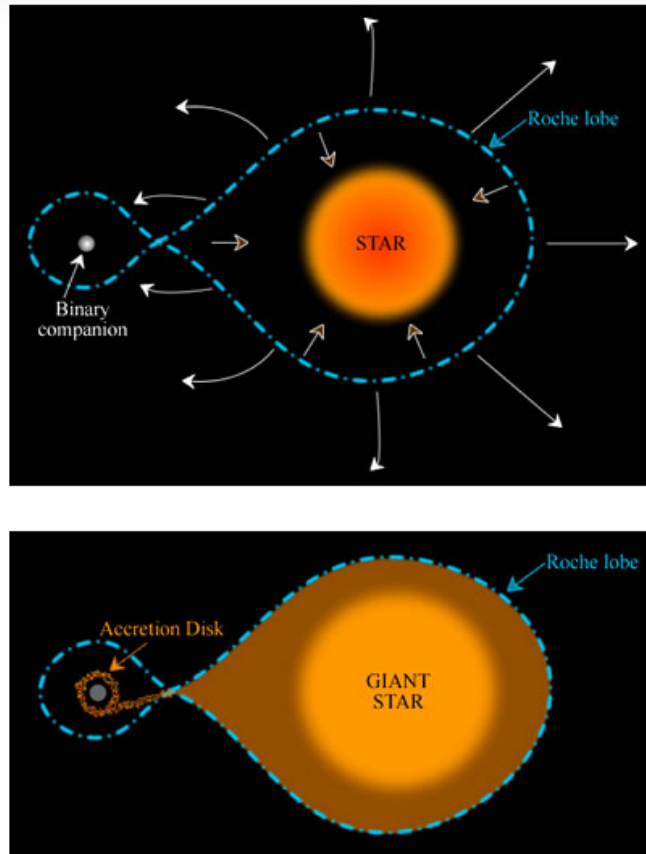


*Image 3: The Roche Lobe and the accretion disk created by the material falling in it. Image source : Swinburne University*

### **Wind-fed accretion**

When the above star does not fill its Roche lobe, but has undergone significant mass loss via its stellar wind, it will result in quasi-spherical accretion. Stellar wind, by definition, is the matter in the form of plasma that is ejected from the upper atmosphere of the star. A neutron star in a relatively close orbit will capture a significant fraction of the wind of these stars, sufficient to power a bright X-ray source.

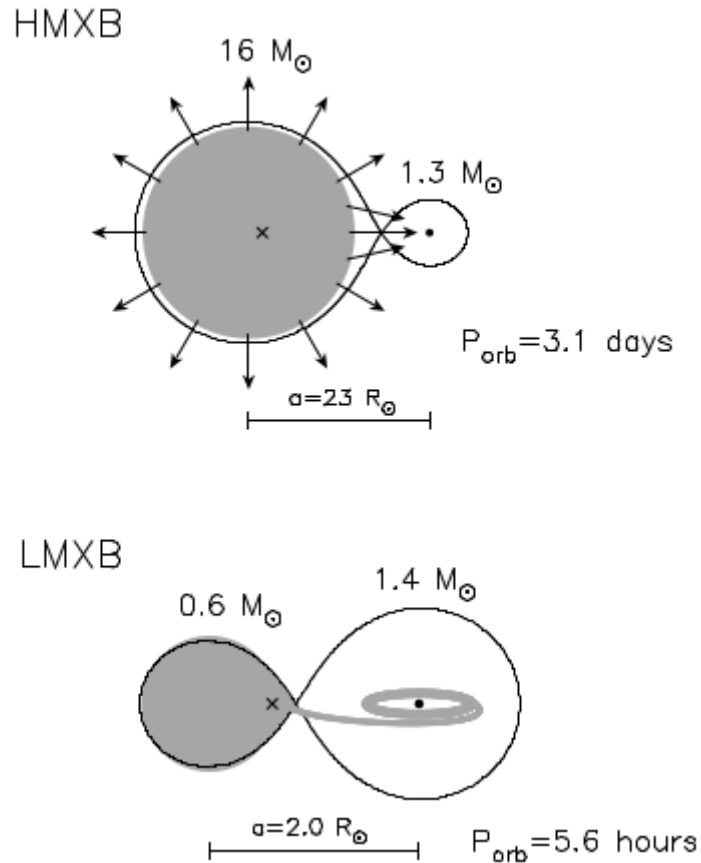


Image 4: Tauris T.M. 7 Van den Heuvel E.P.J(2003)

### Decretion disk

Be stars were discovered around 150 years ago by Secchi(1866) and some of them are among the brightest stars in the sky. Be stars are rapidly rotating and non-radially pulsating B stars forming a decretion disk, which is more precisely an outwardly diffusing gaseous Keplerian disk. Into this category, at first, was all stars that showed a B-type spectrum along with Balmer line emission. An important observational characteristic of these stars is their variability on all time scales.

The emission lines are due to the reprocessing of the optical/UV radiation from the photosphere by the disc. The infrared excess, as well as the polarization as a result of the stellar light being scattered in the disk.

First in the spectral energy distribution of a Be star includes the photospheric emission, the disk emission of reprocessed radiation and disk absorption. Polarimetry provided insights into the nature of the disks of the Be-stars. When the light from the Be-star is scattered by free electrons in the ionized disk, it becomes polarized. For a geometrically thin disk, the polarization direction will be perpendicular to the disk plane.

The spectral lines of Be stars can come from three regions: the star itself, the actual disk, and the circumstellar environment above the disk up to the polar regions. In this work, the analysis was done using the spectrum of the stars and through these the rotational velocities were obtained.

## **2.Methodology**

### **i. Reduction of Stellar Spectra**

The stellar spectra used in this thesis were acquired in the 4.2m William Herschel Telescope in Las Palma Observatory in July 2015. The reduction of the stellar spectra was performed with IRAF. The detailed steps appear in *Appendix 1*.

The reduction of the stellar spectra includes the following steps:

*1.1* Creating an image type. IRAF performs effectively after it can distinguish the files by adding the image type to their headers. The image type relevant for this work are, “bias”, “flat”, “object”, and “arc”.

#### *1.2* Obtaining a Master Bias

Bias frames are zero second exposures obtained with the shutter closed. IRAF will create an average bias image of all the bias taken during the same night, assuming that the bias level has not changed, and then it will be removed from the flat, arc and source frames. For the spectra analysis the whole frame is not needed, only the section that contains the spectra, so first trimming of the images at the important sections is recommended.

#### *1.3* Bias Subtraction and Trimming for arcs, flats and objects.

#### *1.4* Obtaining a master flat and flat-field correction

Flat field accounts for the non uniformity of the sensitivity of the CCD across its surface. The goal is to remove flaws in images that are caused by variations in the pixel-to-pixel sensitivity of the detector and/or by distortions in the optical path. The variations in sensitivity are multiplicative and they need to be divided from the data by removing the pixel to pixel variations. IRAF with the command `Flatcombine` corrects these variations.

The combined flat-field exposures will be normalised across the dispersion axis by dividing it by a polynomial fit.

#### *1.5.*Extraction of the Source Spectrum with `apextract` and `apall` tools of IRAF

*1.6*Wavelength calibration: The next step is the transformation from a pixel to a wavelength scale, that is, to give physical units to the X axis. This is done using the calibration spectrum, meaning the arc images. A calibration or a comparison spectrum is the spectrum taken from a lamp whose content is known. Therefore, the resulting spectrum contains a number of spectra lines whose centers are precisely known. By fitting the wavelength centers of those lines with the position in pixels that they occupy in the extracted spectrum the correspondence between pixels and wavelength(angstroms) can be deduced. Then the identification of the spectra lines follows. Lines that are well distributed along the spectrum pointing them with the cursor and pressing `m` and inserting the actual value which is known from a provided atlas of the lamp.

Once the wavelength calibration is completed, the resulting plot can be examined with `splot`. Then the next step is to normalise the spectrum. Since not the whole spectrum has the same mean value we choose to do that by separating it into two.

After obtaining the spectrum of the stars the next step is to identify which lines are shown.

In order to identify the spectra a given atlas <sup>[6]</sup> is used that contains classified spectra of identified stars and we compare the spectra lines.

## **ii. Spectral Classification**

To classify the stars according to their spectral type. For this, the atlas of Walborn, N. R., & Fitzpatrick, E. L [6], was used to compare standard stars of O and B type with the four stars for this research.

In the spectrum, each line indicates a particular chemical element or molecule, with the line strength indicating the abundance of that element. The comparison was done by the eye by comparing the spectrum obtained from WHT and the atlas. The fact that the spectral type of the optical counterparts of all galactic BeXBs lies in the range O8-B3 helped us restrict our analyses to this relatively narrow range in spectral types.

The most important lines considered for the classification of the stars where for the B0V the weakness in the HeII lines, the CIII and the intensity between the SiV( $\lambda 4116\text{\AA}$ ) and the HeII( $\lambda 4121\text{\AA}$ ) with the triplet of Si IV( $\lambda 4552-68-75\text{\AA}$ ), for the B1-III important factors where the lines C III and O II and how much they blend together and the SiIV lines( $\lambda 4089\text{\AA}$ ,  $\lambda 4116\text{\AA}$ ) and the absence of Helium lines. Last, for the B2 V the appearance of metal lines and their intensity The Si-IV lines, the blending of CIII ( $\lambda 4070\text{\AA}$ ) next to H $\delta$  line and the H $\delta$  line were mostly considered into determining the spectral type of the star.

## **iii. Rotational Velocity**

### **Rotational Velocity**

As mentioned before, Be stars are rapid rotators . According to Townsend et al<sup>[20]</sup>, a possible explanation for the Be phenomenon is, that the equatorial rotation velocities of Be stars are probably close to the critical velocity, for which, material would be easy to “escape” from the star and form a disk around it.

The velocity at the equator of a rotating body where the centrifugal force balances the Newtonian gravity, is the critical velocity. At this rotation rate, mass can be readily lost from the equator and then the circumstellar disk will form.

The quantity that can be measured is the projected rotational velocity,  $v \sin i$ , where,  $v$  is the true rotational velocity and  $i$  is the inclination angle with respect to the line of sight. To measure this three different methods were employed to estimate the rotational velocity of the Be stars: 1) from the width of He I lines, 2) by fitting synthetic spectra to the observed spectra, and 3) through a Fourier transform on the line profiles.

### **Method 1: Full Width at Half Maximum of He I lines**

Steele et al. (1999) performed a study of a sample of 58 Be stars in an attempt to gather a representative sample of Be stars in order to derive their spectral types and rotational velocities. They provide a convenient and easy way to estimate the rotational velocity of a Be star by measuring the FWHM of the best-fit Gaussian to a line profile. The lines used are the He I lines at 4026Å, 4143Å, 4387Å, and 4471Å.

In this method, the tool `splot` of IRAF fitted Gaussian profiles on the He I lines and calculated the Full Width at Half Maximum (FWHM) in each one of these profiles. FWHM is the width measured at half level between the continuum and the peak of the line and then the calibration is performed to obtain the rotational velocities. The measured FWHM was corrected for the instrumental profile.

### **Method 2: Comparison with synthetic spectra**

For the second method the rotational velocities were calculated by comparing the spectra of WHT with a grid of synthetic spectra broadened at different values of rotational velocities. This was done by using the computer program TLUSTY and the package of BSTAR200 to create model atmospheres through SYNSPEC. TLUSTY [17] has been developed for calculating model stellar atmospheres assuming different parameters such as temperature, gravity and rotational velocity. The basic component of the package is TLUSTY, a program for calculating plane-parallel, horizontally homogeneous model stellar atmospheres in equilibrium. The second basic program is SYNSPEC, which is a program for calculating the spectrum emergent from a given model atmosphere. It has been originally designed to synthesize emergent spectra from model atmospheres calculated using TLUSTY. The program is complemented by the program `rotin` which calculates the rotational and instrumental convolutions for the net spectrum produced by SYNSPEC.

The model atmospheres varied with temperatures starting from 15000K to 30000K, gravities with  $\log g = 2$  till  $\log g = 4.25$  and with rotational velocities from  $80 \text{ km s}^{-1}$  to  $320 \text{ km s}^{-1}$ .

The relationship between effective temperature and spectral type was done using the calibration of Pecaut & Mamajek 2013, [7]. We assumed around 30000 for a B0V star, 26000K for a B1-III and for B2V around 22000 K.

### **Method 3: Fourier Transform**

For the third method the projected rotational velocities were determined by applying a Fourier transform to the profile of the spectral lines. This was done following the work of Simón-Díaz, S., & Herrero, A. (2007), [9] who performed a detailed study on how the FT method can be used to determine  $u \sin i$  and how the position of zeroes or the minimum that appear in the graph in this Fourier transform depends on it. The Fourier method of determining the rotational velocity is based on the fact that, between broadening of the lines due to natural or thermal broadenings or other contributions like microturbulence, only with the rotational function minimums will appear and their position will be related to the  $u \sin i$  through this

$$(\lambda/c)u \sin i x_1 = 0.660$$

What is more, in their study Simón-Díaz, S., & Herrero, A. (2007) concluded that the FT method gives consistent results for both metal lines and He lines, so for the spectra used in this thesis again, the He lines were used are the same ones as in the previous methods.

### 3.Results

#### i.Spectral Class

Here are the results of this work. The spectrum of each of the four stars is shown below as well as the significant lines that played a major role in classifying the star.

KS1947, SAX2239.3+6116 – B0V

The spectra for SAX2239 and KS1947 are both filled with hydrogen and helium absorption lines resulting in an early type B stars. Some HeII lines appear weak ( $\lambda 4121\text{\AA}$ ,  $\lambda 4144\text{\AA}$ ,  $\lambda 4541\text{\AA}$ ) which makes them to be a star later than O9 stars and MgII ( $\lambda 4481\text{\AA}$ ) is absent making it a star earlier than a B1. CIII ( $\lambda 4070\text{\AA}$ ) makes it a star closer to B0 and B1. The ratio between the SiV ( $\lambda 4116\text{\AA}$ ) and the HeII ( $\lambda 4121\text{\AA}$ ) with the triplet of Si IV ( $\lambda 4552-68-75\text{\AA}$ ) appearing and, comparing this line next to the HeI ( $\lambda 4471\text{\AA}$ ) favours it to be a B0 spectral class. There are no OII lines which makes the stars to be closer to luminosity class V.

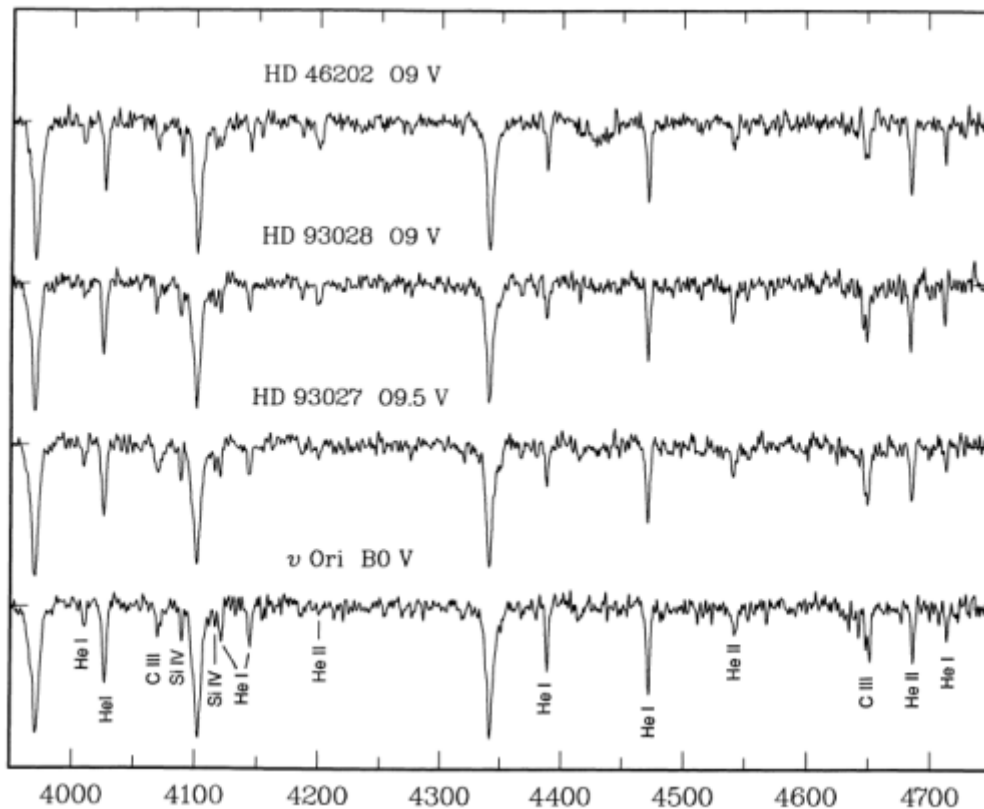


Image 5: The spectral features identifies in  $\nu$  Ori are the Helium lines, C-III blends, Si, and HeII. OB spectral Atlas, Walborn and Fitzpatrick, 1990

### SAX2239

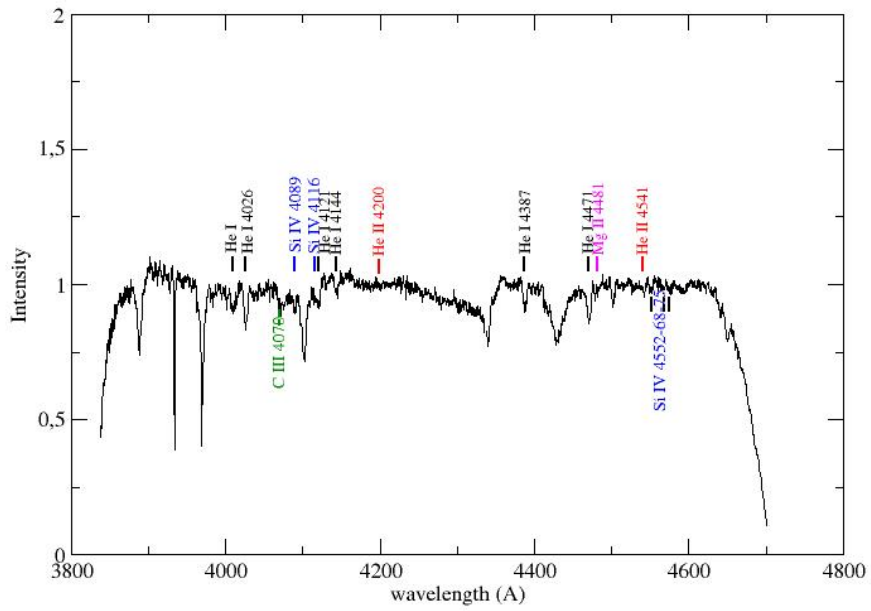


Image 6: The spectrum of SAX2239 with the identification lines for determining it as B0V

### KS1947

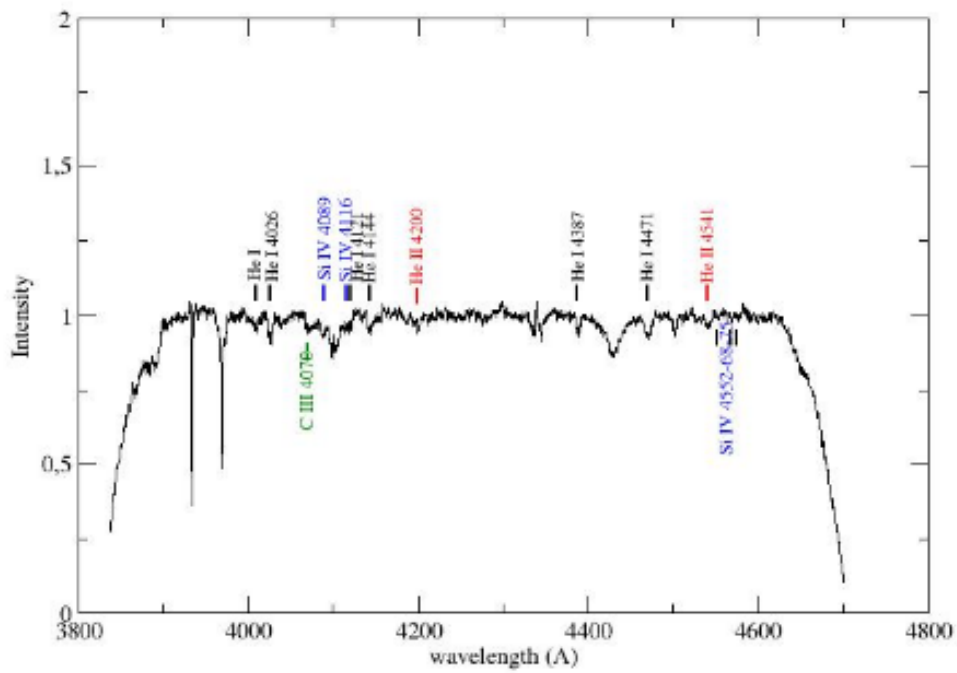
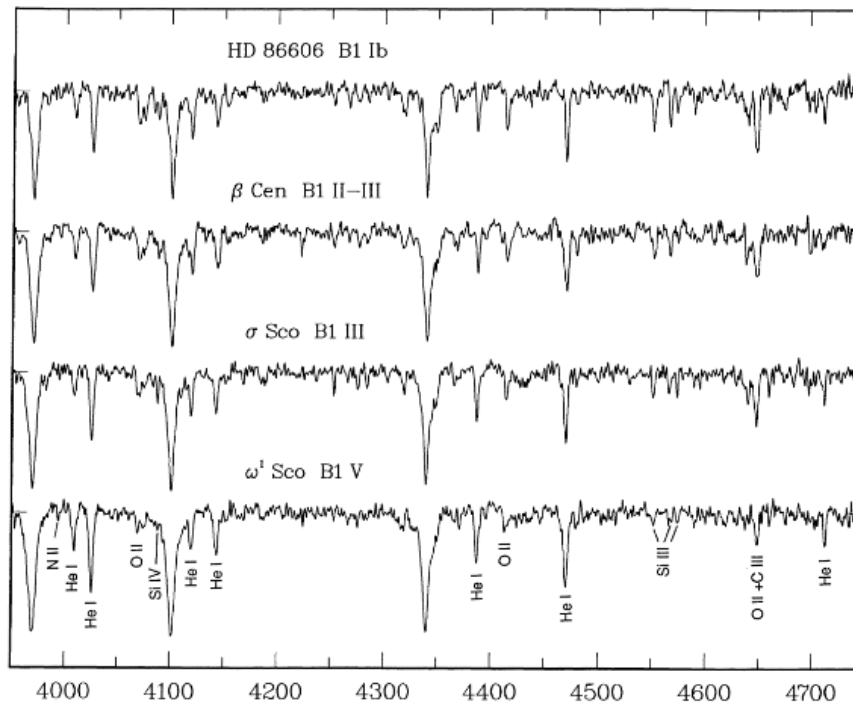


Image 7: The spectrum of KS1947 with the identification lines for determining it as B0V

IGR01363 B1 III

For IGR01363 the main point that helped up identify it as a B1 III were the C III and O II which start to blend together as going from B0 to B1 stars and their two peaks are visible separately which were not in earlier spectral types and they appear to blend together at 4070Å. The intensity comparison for the SiIV lines( $\lambda 4089\text{\AA}$ ,  $\lambda 4116\text{\AA}$ ) next to the emission line of hydrogen as well as the CIII( $\lambda 4070\text{\AA}$ ) make it either a B1 III or a B0.5. The absence of Helium lines, though, indicates that it is a B1 III.



*Image 8: Here the spectral classes are identified by the Si III lines  $\lambda 4552$ / Si IV 4089 and the luminosity classes by Si II  $\lambda 4552$ /He I  $\lambda 4387$ . Important to note the rise of O II line as the luminosity increases. , OB spectral Atlas, Walborn and Fitzpatrick, 1990*

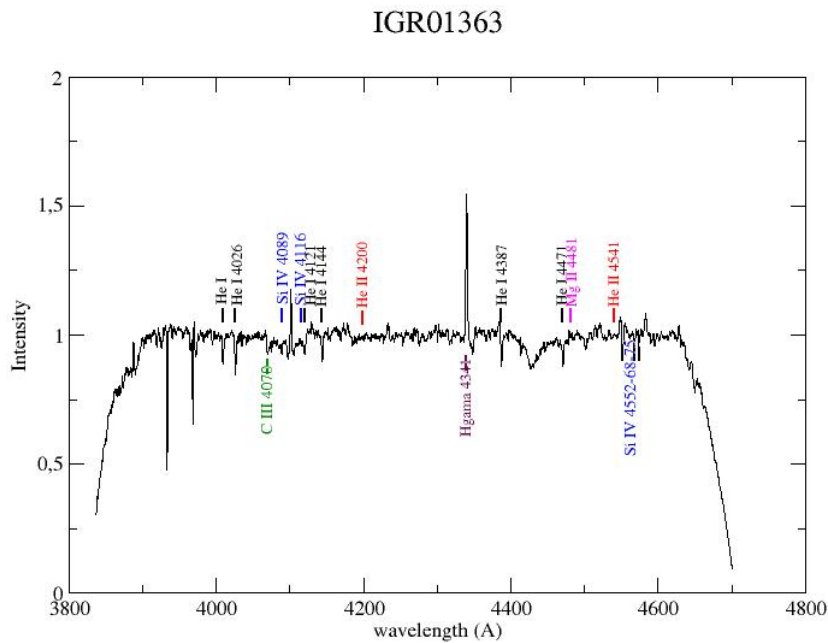


*Image 9: The spectrum of IGR01363 with the identification lines for determining it as B1 III*

IGR01583 B2 V

For IGR01583 the analysis of the spectrum shows hydrogen and helium lines and the identification is done through comparing the metal lines. Going from B0 stars to B2 stars the CIII( $\lambda 4070\text{\AA}$ ) broadens and slightly blends with the H $\delta$  line next to it. The Si-IV lines ( $\lambda 4089\text{\AA}$ ,  $\lambda 4116\text{\AA}$ ) appear rather weak. The Si IV triplet at  $4452-68-75\text{ \AA}$  is seen but weak. The absence of MgII ( $\lambda 4481$ ) makes it rule out either a B2 II, B2 III star or a B1. The intensity comparison of He at  $4121\text{ \AA}$  and at  $4144\text{ \AA}$  favours this star to be B2 V.

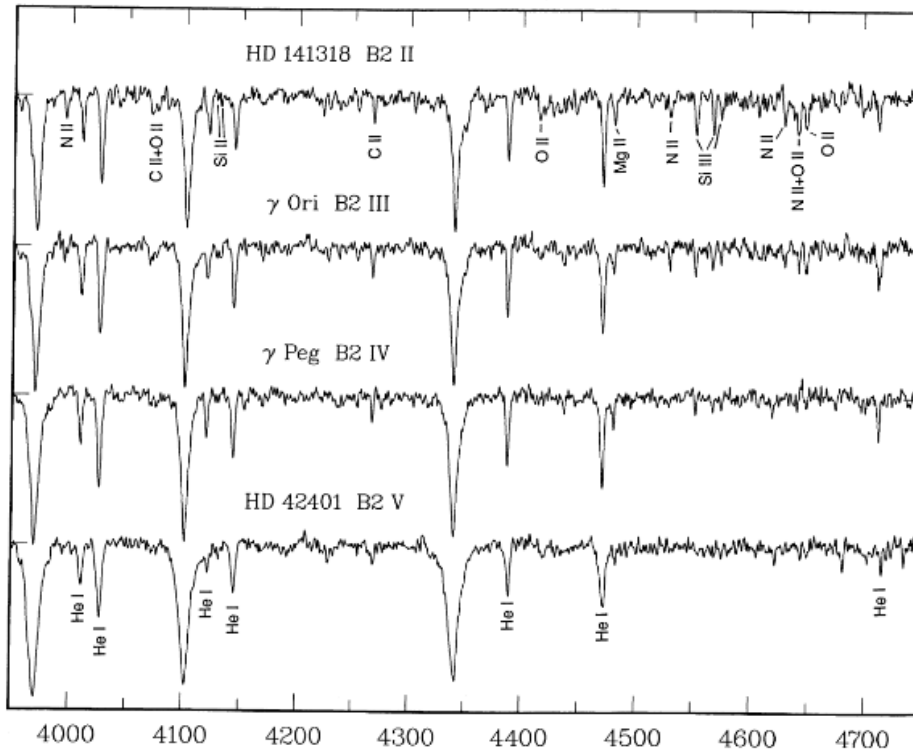


Image 10: Here, the very large He I  $\lambda 4144/\lambda 4121$  ratio is the characteristic of B2 V, OB spectral Atlas, Walborn and Fitzpatrick, 1990

### IGR 01583

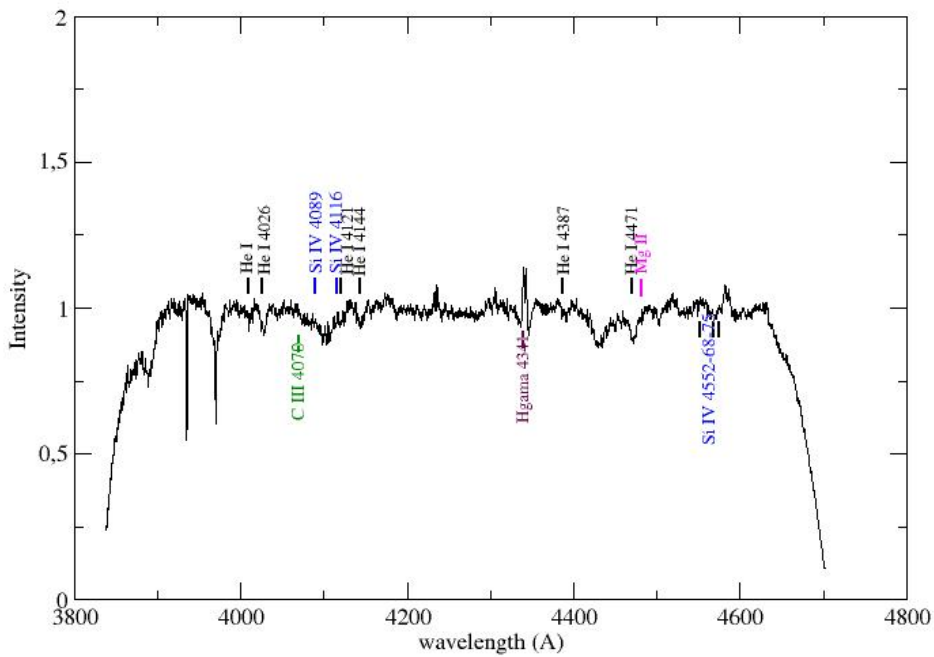


Image 11: The spectrum of IGR01583 with the identification lines for determining it as B2 V

## ii. Rotational velocity

### Method 1: Full Width at Half Maximum of He I lines

The spectral analysis was done using the splot task of IRAF and the spectra was normalised with respect to the local continuum. With splot, we fitted Gaussian profiles on the HeI lines and calculated the Full Width at Half Maximum (FWHM) in each one of these profiles. FWHM is the width measured at half level between the continuum and the peak of the line.

Note that the FWHM has to be corrected for instrumental broadening  $FWHM_{instrumental}$ , which is the FWHM of a very fine line, from the calibration lamp.

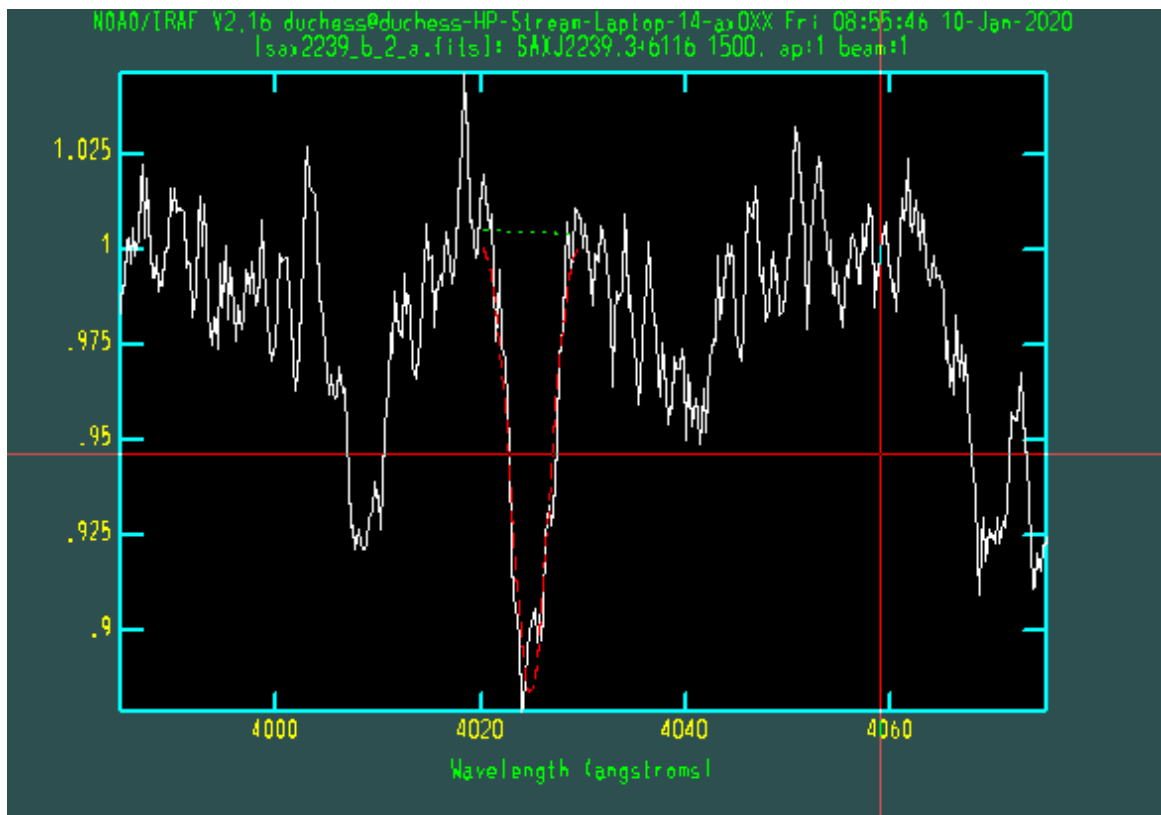


Image 12: Fitting a Gaussian profile on line 4026 of SAX2239

This instrumental correction is performed by this equation:

$$FWHM_{corrected} = \sqrt{((FWHM_{observed})^2 - (FWHM_{instrumental})^2)}$$

Using the calibration of Steele et al. (1999), [8] the fits employed are:

$$\begin{aligned}
 v_{\text{rot}} &= 45.82 F(4026) \text{ km s}^{-1} \\
 v_{\text{rot}} &= 44.51 F(4143) \text{ km s}^{-1} \\
 v_{\text{rot}} &= 42.03 F(4387) \text{ km s}^{-1} \\
 v_{\text{rot}} &= 41.25 F(4471) \text{ km s}^{-1}
 \end{aligned}$$

Where  $F(\lambda)$  is the full width half maximum in Å at a wavelength of  $\lambda$  Å.

We performed five different selection of the continuum in the vicinity of the lines. The final adopted rotational velocity resulted from the average of these five measurements in each line (total 20 measurements), while the error was taken to be the standard deviation.

For each star, the rotational velocity is the mean of all these measurements and their standard deviation was taken as the standard error.

The FWHM was derived directly by the plot tool of IRAF and using the calibration of Steele et al. (1999), the results are:

Star	Rotational Velocity(km/sec)	Standard Deviation(km/sec)
KS 1947+300	300	70
SAX2239.3+6116	210	20
IGR J01583+6713	300	20
IGR J01363+6610	90	8

## Method 2: Comparison with synthetic spectra

For the second method, we first created the synthetic model spectra. This was done using the code Tlusty and Synspec as explained before and with the use of rotin3 the convolved synthetic spectra were obtained. For this, different model atmospheres were used in rotin3 which varied with temperatures starting from 15000K to 30000K, gravities with  $\log g = 2$  till  $\log g = 4.25$  and with rotational velocities from  $80 \text{ km s}^{-1}$  to  $320 \text{ km s}^{-1}$ . After creating the synthetic spectra, I compared it with the ones from the data.

Here, the work was done by first comparing the whole of the spectrum with the whole of the synthetic one, and then secondly only in the wavelengths mentioned in the previous method with range used for each wavelength was 50 to  $100 \text{ \AA}$ , depending on the line. For comparison the chi square test was used to determine whether there is a significant difference between the expected values and the observed values in both of the spectra.

$$\frac{(x_{\text{wht}} - x_{\text{synth}})^2}{x_{\text{synth}}}$$

where  $x_{\text{wht}}$  is the flux of the observed spectrum and  $x_{\text{synth}}$  the flux of the synthetic spectrum, after broadening the line profile wavelength with different values of the rotational velocity using ROTIN3

When using the whole spectrum, the best synthetic spectrum was determined by choosing the one that minimises the sum of the squares of the difference between those two whereas when only parts of it were used, the synthetic spectrum was chosen by the sum of the squares of mean of three regions chosen. The comparisons and the results were made by creating a python sequence for chi chart which is presented in *Appendix 2*.

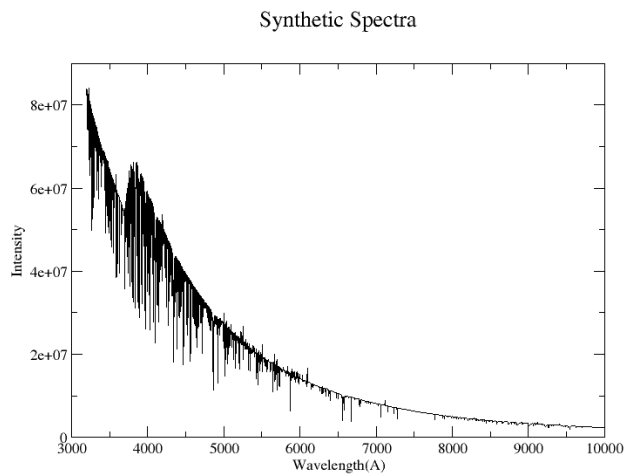


*Image 13: Synthetic Spectra before convolution*

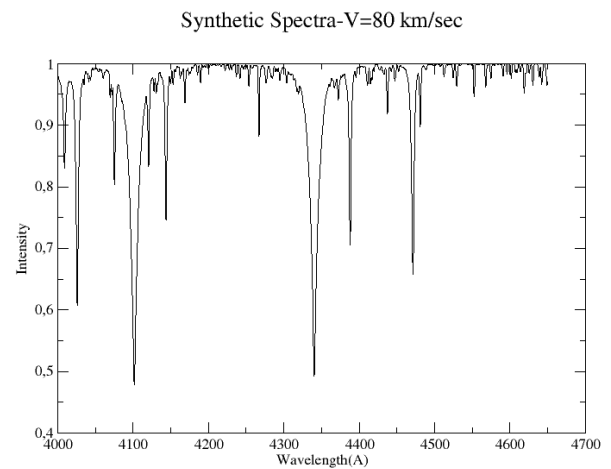


*Image 14: Synthetic Spectra after convolution with a continuum and at a certain velocity*

The comparison was performed first on the whole spectrum and then on narrow wavelength ranges (between 50 and 100 Å) covering the He lines.

Here the plots of the WHT spectra(black) along with the synthetic spectra appear(colourful)

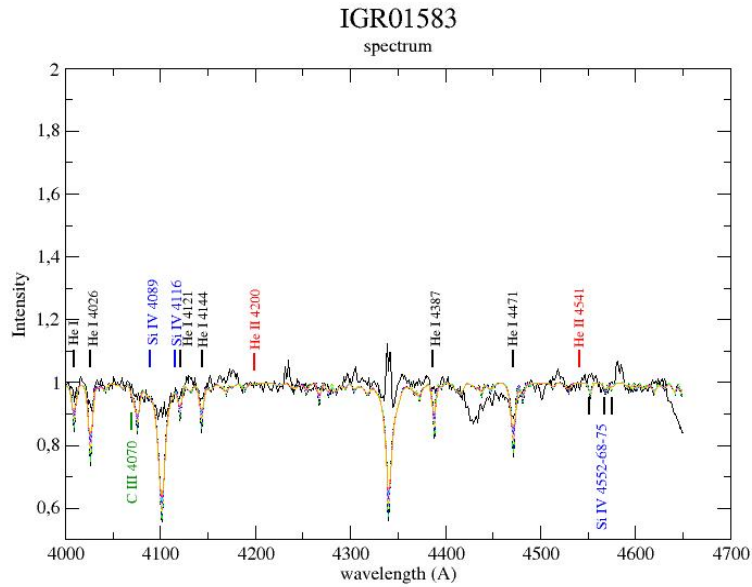


*Image 16: The spectrum of IGR01583 (black) compared to the synthetic spectra derived from ROTIN3 (colourful) for different rotation velocities of the same temperature, 22000K*

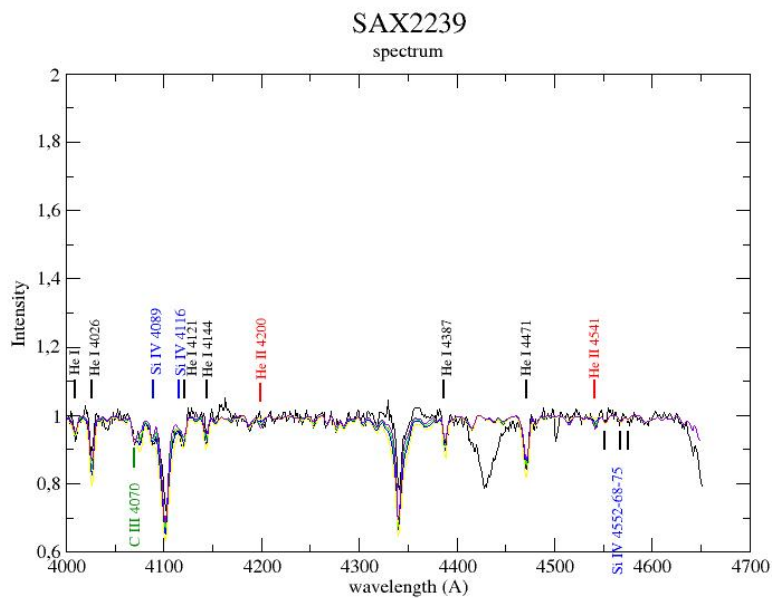


*Image 17: The spectrum of SAX2239 (black) compared to the synthetic spectra derived from ROTIN3 (colourful) for different rotation velocities of the same temperature, 30000K*

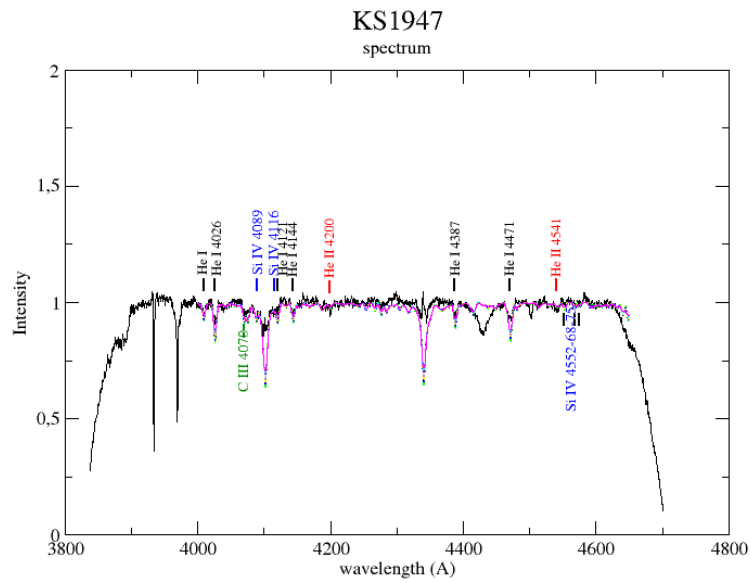


*Image 18: The spectrum of KS1947 (black) compared to the synthetic spectra derived from ROTIN3(colourful) for different rotation velocities of the same temperature, 30000K*

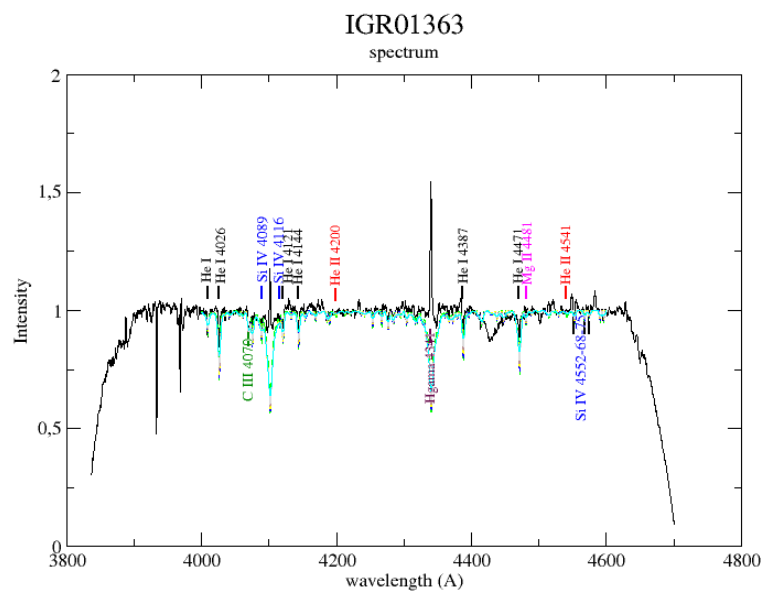


*Image 19: The spectrum of IGR01363 (black) compared to the synthetic spectra derived from ROTIN3(colourful) for different rotation velocities of the same temperature, 25000K*

The results of the chi-comparison are presented in the following tables,

First comparison-all of the spectrum of the WHT spectra with the synthetic ones:

Star	Rotational Velocity(km/sec)	Standard Deviation(km/sec)
KS 1947+300	320	20
SAX2239.3+6116	240	20
IGR J01583+6713	320	20
IGR J01363+6610	170	20

Second comparison-the spectrum of each line of the WHT spectra with the synthetic ones(average for each x-binary star for all the lines):

Star	Rotational Velocity(km/sec)	Standard Deviation(km/sec)
KS 1947+300	320	20
SAX2239.3+6116	240	20
IGR J01583+6713	320	20
IGR J01363+6610	200	20

### Method 3: Fourier Transform

To determine which part of the continuum gives a better result, a convolved spectra that was derived from ROTIN3 and the previous method was used as this synthetic spectra does not suffer from emission or other kinds of broadening. Furthermore, for this synthetic spectra the rotational velocity it represents was already known. Two graphs for this test appear below with different length range on the continuum of the line.

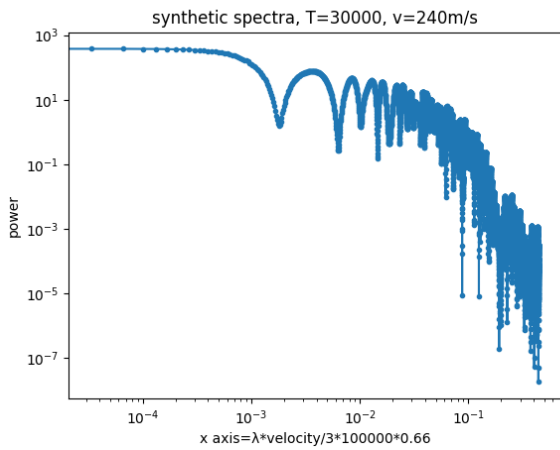


Image 20: FT transformation on synthetic spectra at  $T=30000\text{K}$ ,  $v=240\text{km/sec}$ , long range in wavelength, calculated  $v=614\text{km/sec}$ (for the first infinite zero)

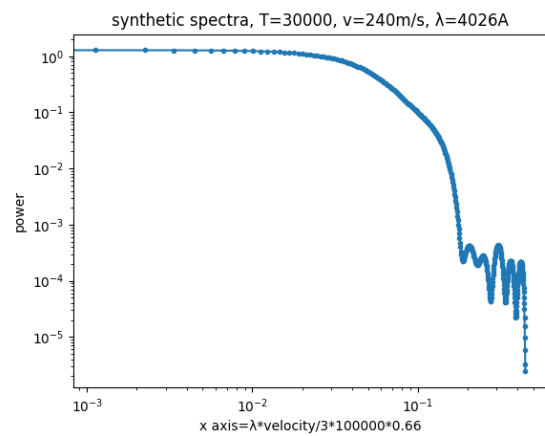


Image 21: FT transformation on synthetic spectra at  $T=30000\text{K}$ ,  $v=240\text{ km/sec}$ , short range in wavelength, calculated  $v=258\text{km/sec}$

It is obvious that better and more accurate results appear the closer to the line the range is chosen while when it is affected by the line preceding the chosen one, the more minimums appear and the more the transformation is affected by them.

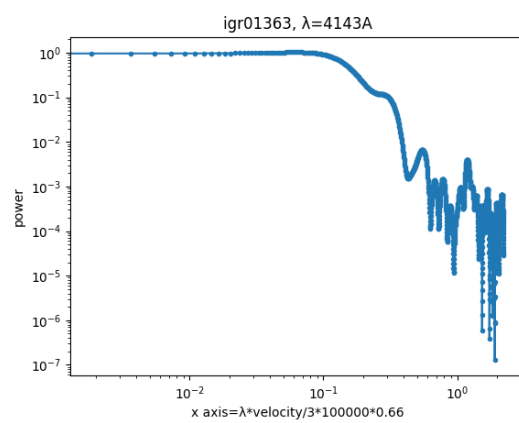
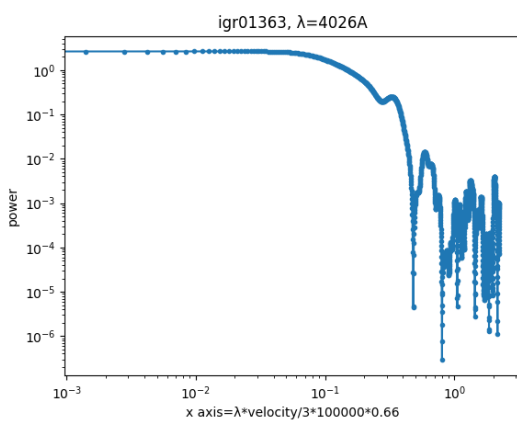
Consequently, for the Fourier transformations of the WHT, the chosen range to do was  $30\text{\AA}$  depending on the line and its broadening.

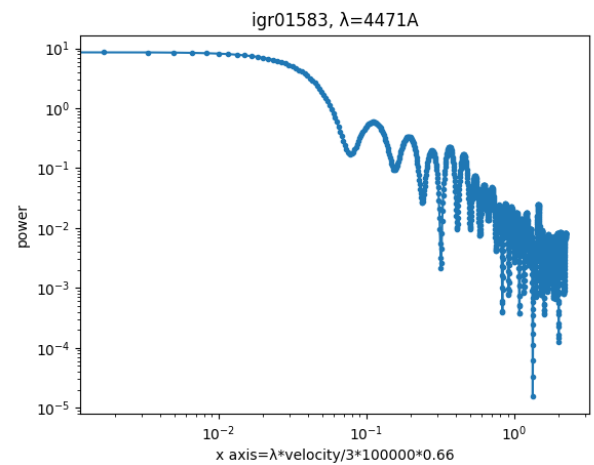
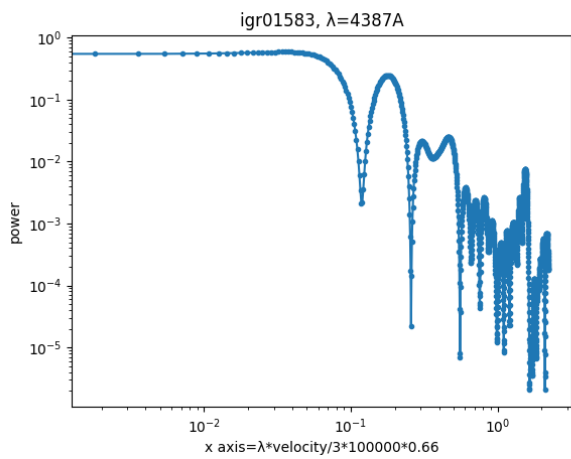
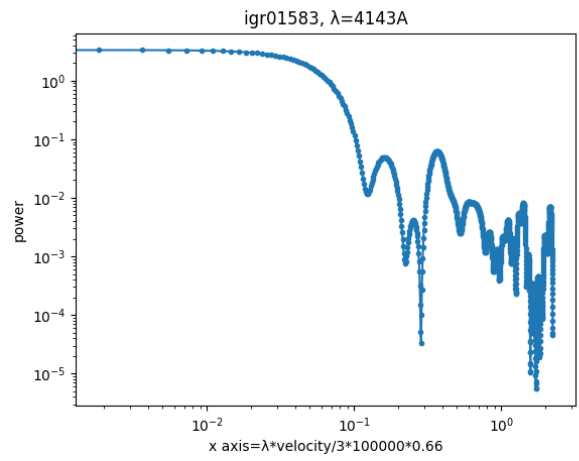
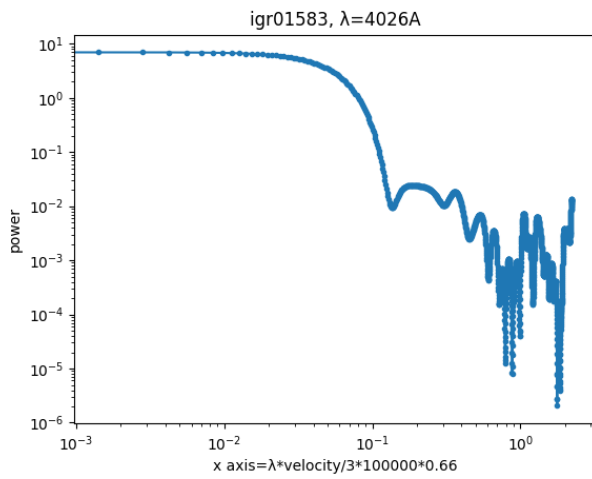
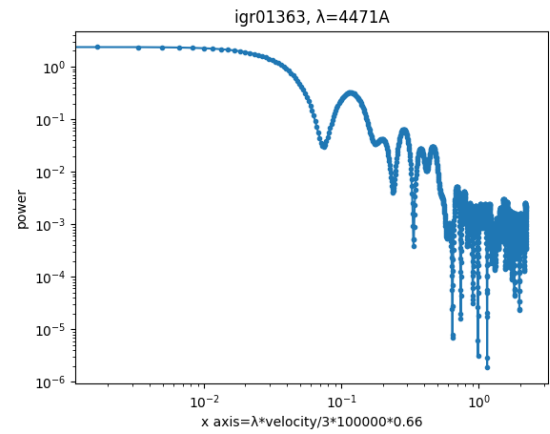
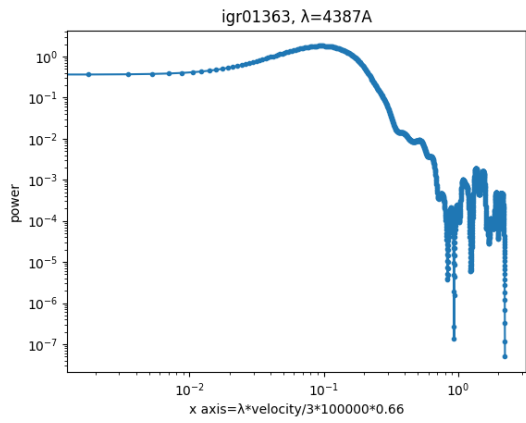
The Fourier transformation was performed with the Fourier transformation done with a python script as presented in appendix.

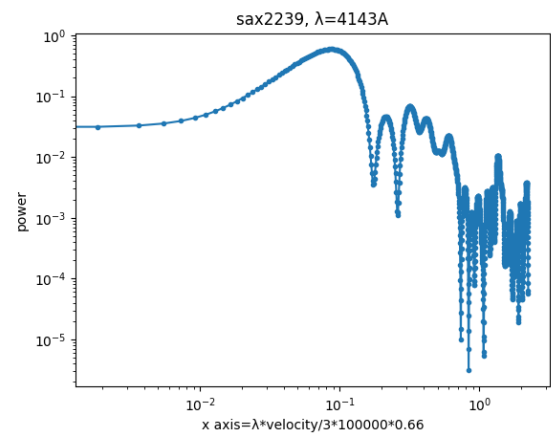
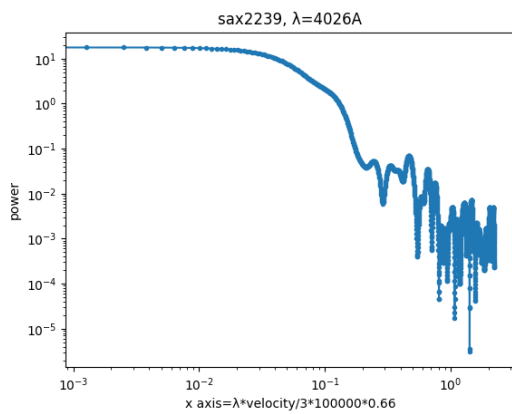
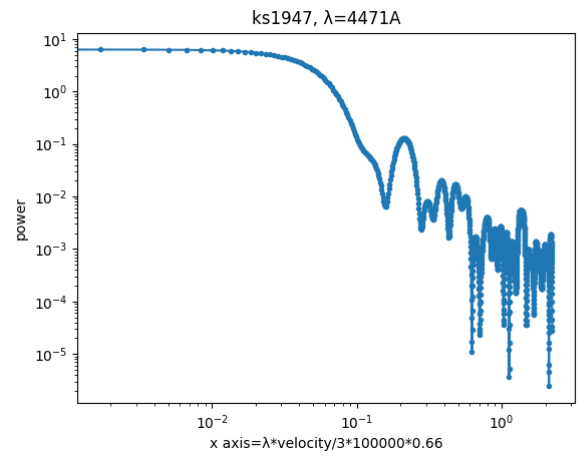
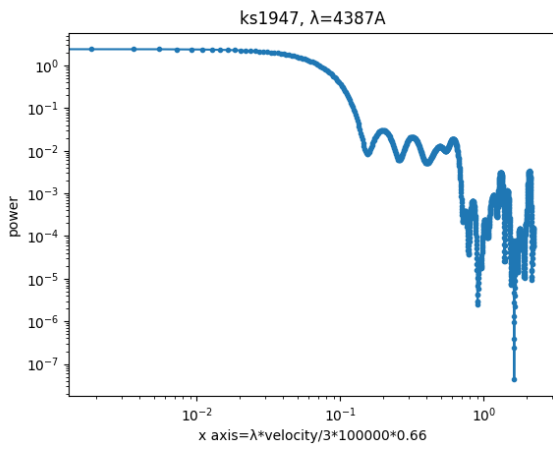
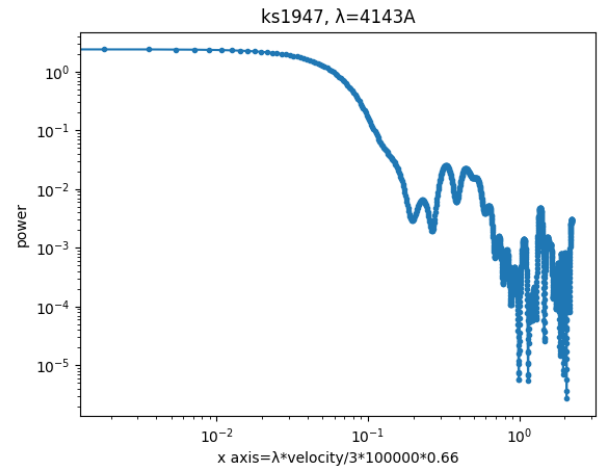
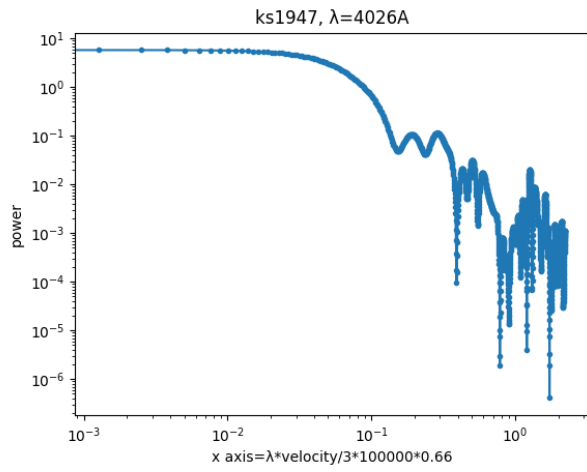
In the x axis the “zeros” or “minimums” appear. The first minimum will determine the rotational velocity as:

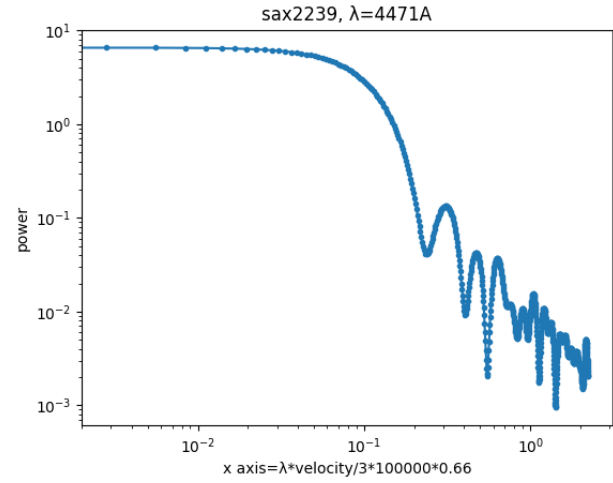
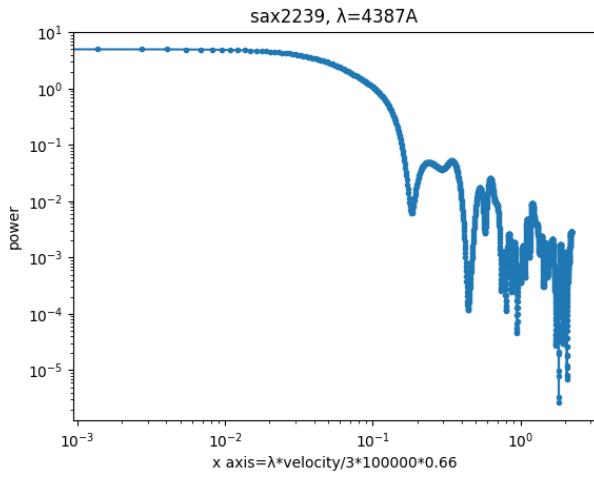
$$v=3*100000*0.66/(\text{wavelength}*x_{\text{axis}})$$

For each star and the fourier transformation around each line is shown below.









*Images 22-31: FT on a range of the spectra for all studied stars*

The results after converting the “zeros” into velocities are below:

Star	Rotational Velocity(km/sec)	Standard Deviation(km/sec)
KS 1947+300	250	80
SAX2239.3+6116	250	20
IGR J01583+6713	380	90
IGR J01363+6610	100	30

### **Comparison of the rotational velocities of the three methods**

In the table below it is clear that more or less the three methods give the same results for the rotational velocity.

Star	Rotational Velocity(km/sec ) through FWHM	Rotational Velocity(km/sec) through Rotin3 (full spectrum)	Rotational Velocity(km/sec) through Rotin3 (average for all lines)	Rotational Velocity(km/sec) through Fourier Transformaton
KS 1947+300	300±70	320±20	320±20	250±80
SAX2239.3+6116	210±20	240±20	240±20	250±20
IGR J01583+6713	300±20	320±20	320±20	380±90
IGR J01363+6610	90±8	170±20	200±20	100±33

## **4.Discussion**

### **Issues due to strong emission**

The observed spectrum of Be stars is a combination of the spectrum produced by the photospheric absorption of the Be star and by the emission due to its circumstellar disk. Since the strength of the emission increases with the size of the disk, systems with large disk may affect the shape of the spectral lines, even those that are not normally affected in smaller disk, such as the Helium lines. The equivalent width of the H $\alpha$  line in IGR J01583+6713 and IGR J01363+6610 is -48 and -62, respectively. For KS 1947+300 is -10 and for SAX2239.3+6116 -0.58. Therefore, we expect our results to be affected by this strong emission, especially for IGR J01583+6713 and IGR J01363+6610. Ideally, the determination of the spectral type and the rotational velocity should be done during a disk-loss episode. This illustrates the importance of monitoring programs to follow the spectral variability of BeXBs.

### **Spectral Class**

Negueruela I. in his paper of the nature of Be/Xray binaries [23] studied the population between Be stars and Be stars that belong to a binary system. In his study he concluded that it is unlikely for BeX/Ray binaries that emit in optical is going to fall to a later spectral type than B2. Our results seem to be coherent with his conclusion as the stars were categorised as B0V, B1-III and B2-V.

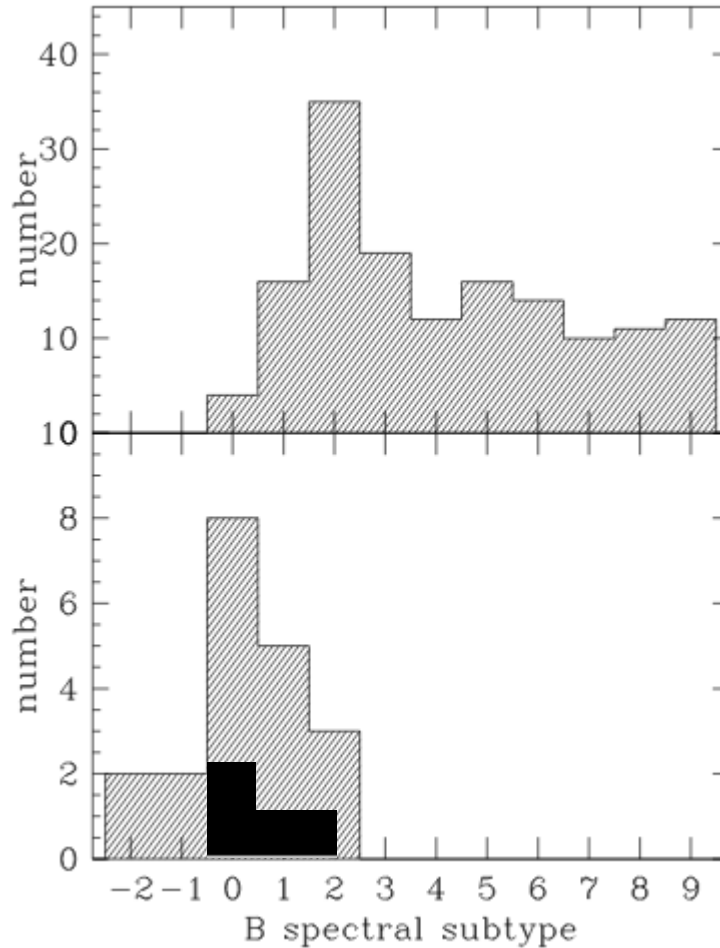


Image 33: Dashed lines is the whole sample, black for IGRJ01363+6610, IGR J01583+6713, SAX2239.3+6116, and KS 1947+300+300. Comparison between the spectral types of Be Binary stars(top panel) and BeX binary stars(bottom panel) , sample taken from Negueruela (1998)

## Rotational Velocities

The determination of the rotational velocity in Be stars is important because it is thought to be linked with the formation of the circumstellar disk, which is still an open question in the field. Also, knowing the rotational velocity help setting constraints on the velocity law and density of the circumstellar disk, as explain below.

Further observations and research on other parameters such as the H $\alpha$  line (FWHM, peak separation in double peaked profiled that at this work, the data acquired did not have) can reveal, as based on similar studies of Be stars (Hanuchik et al, 1988) that the velocity profile of these stars can be correlated with the circumstellar disk. This correlation can be expressed as a disk velocity law as

$$v_{\text{rot}} = v_* \left( \frac{R_*}{r_d} \right)^j ,$$

where  $u_*$  and  $R_*$  are the star rotational velocity and radius and  $j$  is the disk rotational velocity parameter, which may adopt three values 1, -1, 0.5.

For  $j=1$ , is the case of conservation of angular momentum, where the circumstellar gas has the same angular momentum per unit mass as at the stellar surface.

For  $j=-1$  corresponds to the rigid rotation which might happen in the innermost regions of the disk and for  $j=0.5$  is a Keplerian disk.

The index  $j$  can be estimated by the following law:

$$\log\left(\frac{\Delta V}{2v_* \sin i}\right) = -a \log(-EW(H\alpha)) + b,$$

In this case,  $a = j/2$  and  $b$  is related to the electron density in the disk (Hanuschik et al. 1988). From a sample of 93 isolated Be stars of all spectral types Hanuschik (1989) found  $a = 0.32$  and  $b = -0.20$ . This calculation was repeated using the IPHAS list of isolated Be stars and fitting this data with the equations gave  $a = 0.24 \pm 0.11$  and  $b = -0.15 \pm 0.12$ . For the IPHAS sample of classical Be stars,  $j \approx 0.5$ , as expected for a Keplerian disk. (Steele et al, 1999)

Further studies on these, on BeXR binaries show that they indeed follow a linear regression while studies on BeX stars that are not part of a binary system, indicate a less denser disk than the ones who belong on a binary system as it can be seen in images 34, 34, (Reig(2016) [21])

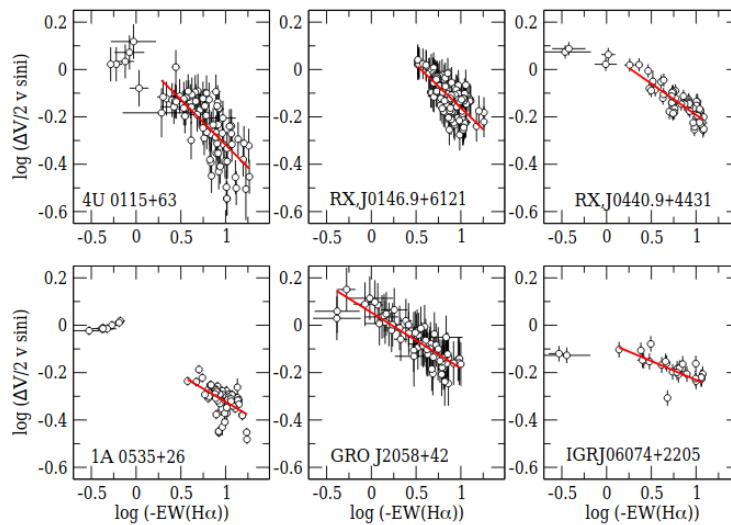


*Image 34: Correlation between the peak separation and the H $\alpha$  equivalent width for six BeXBs. The line represents the best fit to a linear regression(Reig, 2016)*

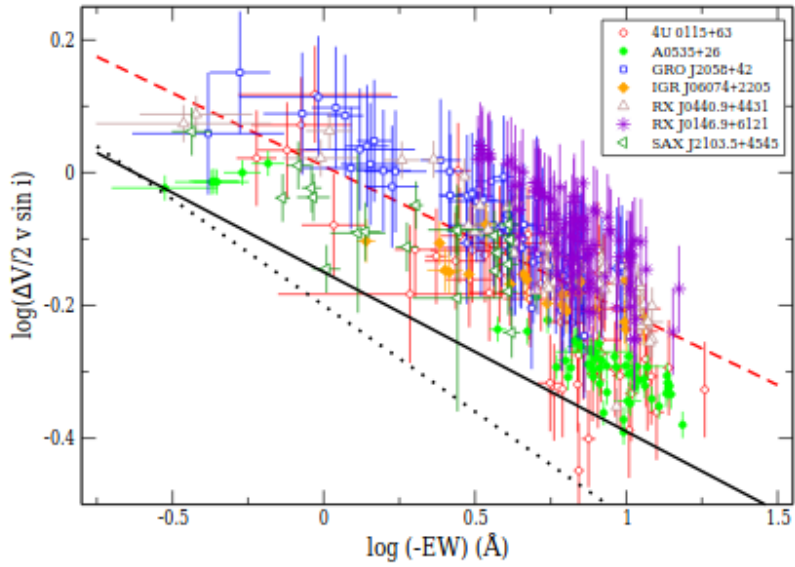


Image 35: Relationship between the peak separation and the H $\alpha$  equivalent width. The solid and dashed line represents the average behaviour of 30 classical Be stars with spectral type in the range O9–B3 (Gkouvelis et al. 2016b) and 93 Be stars of all spectral types (Hanuschik 1989), respectively. BeXBs lie systematically above the Be stars' line (Reig, 2016) [21]

Furthermore, comparing the results of studied stars with the sample of Steele et al., they all fall into the velocity range according to the luminosity class. KS 1947+300, SAX 2239.3+6116, IGR J01583+6713 obtain velocities of over 200 km/sec for every method analysed and IGR J01363+6610 around 100 km/sec

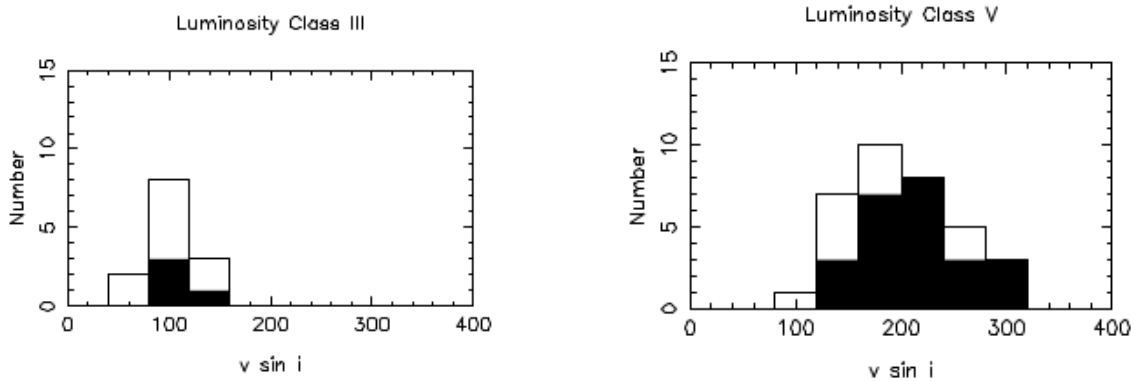
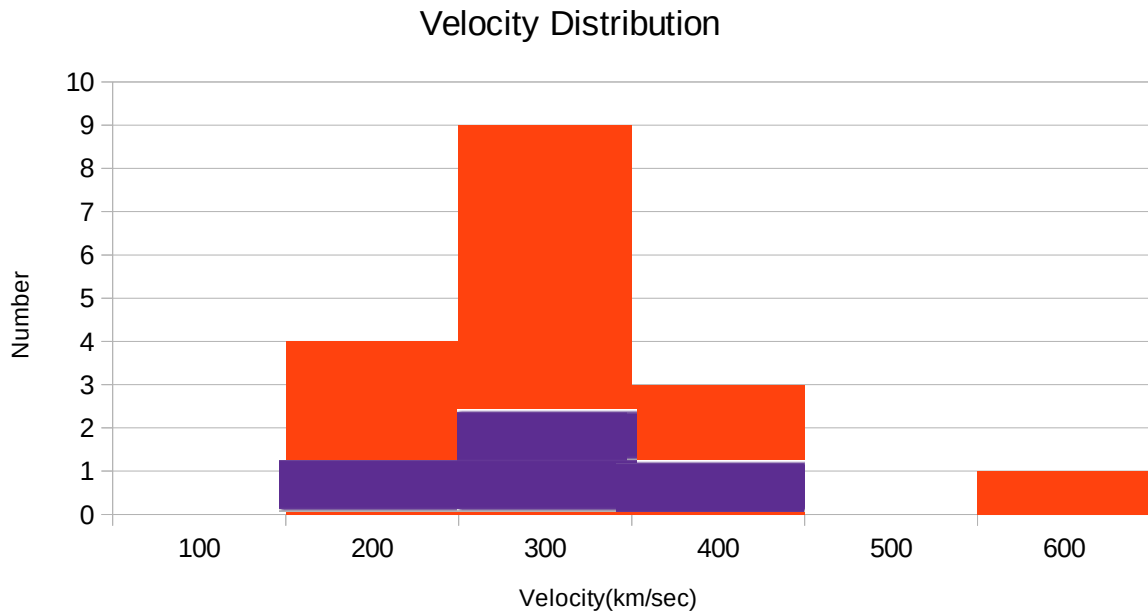


Image 36&37:  $v \sin i$  distributions for all objects in the sample (hollow plus filled areas) and objects in a volume limited subset of the sample (filled area only), Steele et al, 1999



*Image 38: Red is the whole sample, blue for IGRJ01363+6610, IGR J01583+6713, SAX2239.3+6116, and KS 1947+300+300. The distribution of velocities of a sample of BeX binary stars , sample taken from Reig P. & Fabregat, J.(2015)*

Also, comparing the four X-ray Binaries that were analysed in this work to a sample of 15 other BeX binaries from the work of Reig P. & Fabregat, J.(2015), it is still obvious that they fall into the velocity range for these stars.

### Critical Velocity and inclination angle

For a star the critical velocity is given by:  $v_c = \sqrt{GM_*/R_e} = \sqrt{2GM_*/3R_p}$ ,

where the 'e' and 'p' subscripts are used throughout to denote equatorial and polar values, respectively (we assume uniform angular velocity at the stellar surface).

Using this equation Townsend et al, 2004 calculated the critical velocities for different spectral types. The results for 5 of the spectral types he studied are presented below.

Sp. Subtype	$M_*$ ( $M_\odot$ )	$R_p$ ( $R_\odot$ )	$v_c$ ( $\text{km s}^{-1}$ )	$\log L_*$ (dex $L_\odot$ )
B0	17.5	7.7	538	4.64
B0.5	14.6	6.9	519	4.41
B1	12.5	6.3	502	4.21
B1.5	10.8	5.7	491	4.01
B2	9.6	5.4	475	3.85

*Image 38: Parameters for calculating the critical velocity of B-type stars, Townsend et al, 2004*

If we assume that the Be star is rotating at the critical velocity, then we can set a lower limit on the inclination  $v_{\text{rot}} \sin i = v$ , so  $\sin i = v/v_{\text{crit}}$ ,  $\sin i < v/v_{\text{crit}}$  where  $v$  is the measured value.

Star	Inclination angle ( <i>degrees</i> )	Average of Rotational Velocities ( <i>km/sec</i> )
KS 1947+300	34°	300
SAX2239.3+6116	25°	235
IGR J01583+6713	29°	330
IGR J01363+6610	17°	140

## **5. Conclusion**

In conclusion, in this work, I carried out a spectral analysis of four BeXBs. From the 3900-4500 Å spectral range, I derived the spectral class of KS 1947+300, SAX2239.3+6116, IGR J01583+6713 and IGR J01363+6610 for the first time. From the shape of four Helium lines, I also estimated their rotational velocities using three different methods. The three methods provided values that agreed within the uncertainty, except for IGR J01363+6610. I speculate that the reason for this disagreement is the strong emission that results from a large circumstellar disk, in combination with the fact that this source shows the narrowest lines.

## 6.Appendix

### Python Script 1- putting all data under chi test and finding the best value

```
import math

thList=[]
with open('compare.lis','r') as th:
    for line in th:
        thList.append(line.split())

for exp in
['igr01583_1.dat','igr01583_2.dat','igr01363_1.dat','igr01363_2.dat','ks1947_1.dat','ks1947_2.dat','sa
x2239_1.dat','sax2239_2.dat']:
    minelist=[]
    with open (exp,"r") as mine:
        for line in mine:
            minelist.append(line.split(" ")[1][0:-2])

average=[]
for i in thList:
    comparelist=[]
    with open (str(i[0]), "r") as compare:
        for line in compare:
            comparelist.append(line.split()[1])

    #x for mine y for compare
    comp=[]
    for i,j in zip(minelist,comparelist):
        comp.append(math.pow((float(i)-float(j)),2)/float(i))

    average.append(sum(comp)/len(comp))

mini=average[0]
p=0
for i in range(len(average)):
    if average[i]<mini:
        mini=average[i]
        p=i
with open('result.dat','a') as out:
    out.write('{} {} {} \n'.format(exp,thList[p][0],mini))
```

## Python Script 2- binning procedure to fix the continuum

```
import math

def aver5(a1, a2, a3, a4, a5):
    sum = a1 + a2 + a3 + a4 + a5
    return sum/5

def readNwrite(file_to_read, file_to_write):
    fread = open(file_to_read, "r")

    if fread.mode == 'r':
        contents = fread.read()

    words = contents.split()
    size = len(words)

    fwrite = open(file_to_write, "w+")

    i=0
    while (i+10 < size):
        xs = aver5(float(words[i]), float(words[i+2]), float(words[i+4]), float(words[i+6]),
float(words[i+8]))
        ys = aver5(float(words[i+1]), float(words[i+3]), float(words[i+5]), float(words[i+7]),
float(words[i+9]))
        fwrite.write("%f " % xs)
        fwrite.write("%f\r\n" % ys)
        i = i+10

#Main

arxeiaIN = open("arxeia.lis", "r")
arxeiaOUT = open("arxeia_binned.lis", "r")

if (arxeiaIN.mode == 'r') and (arxeiaOUT.mode == 'r'):
    conIN = arxeiaIN.read(); conOUT = arxeiaOUT.read()

files_in = conIN.split()
files_out = conOUT.split()
size = len(files_in)

for i in range(0, size):
    readNwrite(files_in[i], files_out[i])
```

## Python Script 3- Fourier Transform

```
import matplotlib.pyplot as plt
import numpy as np
import math

t,y = np.loadtxt("star_1_l1.dat",skiprows=0,unpack=True)

#stars: ks1947, igr01363, igr01583, sax2239
#wavelengths(l): 4026, 4143, 4387, 4471,
plt.plot(t, y, "-")
plt.xlabel("Wavelength")
plt.ylabel("Intensity")
plt.show()

y = y - 1.0

n = len(t)
freq=np.fft.rfftfreq(n,d=t[1]-t[0])
power = np.abs(np.fft.rfft(y,n))**2

nn = 50*len(t)
freqs=np.fft.rfftfreq(nn,d=t[1]-t[0])
powers = np.abs(np.fft.rfft(y,nn))**2
#powers2=math.log(powers, 10)
#xaxis=3*100000*0.66/(4026*powers2)

plt.plot(freqs, powers, "-")
plt.title("sax2239, λ=4471A")
plt.xlabel("x axis=λ*velocity/3*100000*0.66"); plt.ylabel("power")
plt.xscale("log")
plt.yscale("log")
plt.show()
```

# Reduction of Stellar Spectra with IRAF

In Appendix 4 there is a step by step guide dedicated to spectroscopic data reduction is presented which can be used as a tool to handle raw data and obtain accurate stellar spectra using IRAF. These are the exact steps followed in order to reduce the data given of the William Hershel Telescope.

## 1.1 Creating an image type

IRAF performs effectively after it can distinguish the files by adding the image type to their headers. If this is not done automatically during the night of the observation it is necessary to be done now.

The different image types are:

object:the file containing the source images

zero:the file containing the bias images

dark:the file containing the dark count images

flat:flat field images

comp:comparison or arc images

illum:illumination images

fringe:fringe correction images

other: other image types defines in the translation file

none:images without an image type parameter

unknown: image types not defined in the translation file

NOTE : for IRAF to identify the image correctly, type:

load package noao and ccdred

Now, that iraf has loaded the correc package:

ccdred>setins and choose "direct".

If IRAF does not have the image type, problems will occur during the analysis of the data as it will not be able to understand what kind of file it is loading, which will be needed later in the process.

To add the image type in the data files:

1. he first step is to create different lists for the different image types that are going to be used in the analysis. For the data of WHT these were flats, objects, bias and arcs and the lists will contain the names of the respective categories. (eg fltr0001.fit is a flat image, so it goes to flatb.lis) For the data used in this analysis the arcs, flat, bias and data images were both in the blue and the red spectrum each one needs a different list

Creating a list by typing: ecl> files data\*.fit >data.lis

This will collect all the files containing the string data and put them in the same list.

2. To add the image file in all the files of the list type:

ecl>ccdredit @flat.lis IMAGETYP

NOTE: if we have frames with different slit sizes or obtain at different part of the spectrum(such as red and blue), it is necessary to create different lists for each one of them. The following steps will be carried out for each one of them.

The image header of the fits files contains the information of the image type and with the following command in the terminal this can be checked. !more "filename" (filename to be the name of a fit file eg flat-001.fit)

3. Creating different lists for bias, arcs and flats naming them

- flats\_r.list, the flat images in the red part of the spectrum
- flats\_b.list, the flat images in blue part of the spectrum
- arcs\_r.list, the arc images in the red part of the spectrum
- arcs\_b.list, the arc images in the blue part of the spectrum
- bias\_r.list
- bias\_b.list
- objects\_r.list
- objects\_b.list

In the above lists when it was necessary to create new lists with the images taken from the previous lists, the suffix `_s` contained the trimmed and `_x` for the final spectrum.

## 1.2 Obtaining a Master Bias

Bias frames are zero second exposures obtained with the shutter closed. This step will create an average bias image of all the bias taken during the same night, assuming that the bias level has not changed, and then it will be removed from the flat, arc and source frames. For the spectra analysis the whole frame is not needed, only the section that contains the spectra, so first trimming of the images at the important sections has to be done. The steps to do this are:

1. Load the package that is able to do so(ccdred) : `ecl>noao.imred.ccdred`
2. Create a master bias frame with “zerocombine” : `ecl>zerocombine @bias.list`  
`output=bias_combined.fits`

`Bias_combined.fits` is the Master Bias image. There was a different bias for blue and a different one for red.

## 1.3 Bias Subtraction and Trimming

1. The tool to subtract the average bias from all the arcs, flats and objects is `ccdproc`:  
`ccdproc images=@flat.list output=flat_s.list ccdtype=flat fixpix=no oversca=no trim=yes`  
`zerocor=yes zero=bias_combined.fits darkcor=no flatcor=no illumco=no fringece=no readcor=no`  
`scancor=no biassec=[0:0,0:0] trimsec=[x1:x2,y1:y2]`

**IMPORTANT:**

The suffix `_s` denotes to the trimmed images.

The images parameter has to have the appropriate list.

`x1`, `x2`, `y1`, `y2` are the pixel numbers that define the subregion of the CCD image that needs to be extracted. To obtain the numbers the procedure is to open an image with the spectra with the `ds9` tool. Make sure the orientation is correct and check which will be the borders for trimming. Check where the slit is located. For `y1`, `y2` use values `+100` and `-100` of the actual value and for `x1`, `x2` the actual values where the slit starts and finishes. The trim section is the same for every slit size.

Now the previous steps are repeated for arcs, flats and objects.

## 1.4 Obtaining a master flat

Flat field accounts for the non uniformity of the sensitivity of the CCD across its surface. The goal is to remove flaws in images that are caused by variations in the pixel-to-pixel sensitivity of the detector and/or by distortions in the optical path. The variations in sensitivity are multiplicative and they needed to be divided from the data by removing the pixel to pixel variations. Flatcombine corrects these variations.

In the package noao>imred>ccdred :

1.Flatcombine [input=@flat\\_s.lis](#) output=flat\_av.fit combine=average scale=mode reject=avsigclip ccdtype=flat delete=no rdnoise=5.95 gain=0.989 process=no

2.This process is done for all the different flats we have (eg in blue or red).  
By typing “bye” the process is back to ecl and for the normalisation a new package is loaded  
noao>twodspec>longslit

3. The combined flat-field exposed will be normalised across the dispersion axis by dividing it by a polynomial fit with the tool “response” :

>ecl epar “response”

Now a graphic environment will appear that is user friendly and easier to plug in the following values:

calibrat=flat\_av.fit normaliz=flat\_av.fit response=flat\_an\_norm.fit interac=yes functio=spline3  
order=8 low\_rej=3 niterat=1

Save the parameters and in the terminal type

>response

and then press *enter* until the output appears on the screen. Then “q” for exit.

## 1.5 Flat-field correction

Load the package noao>imred>ccdred to correct the flat-field from the source images :  
ccdproc [images=@objects\\_s.lis](#) [output=@objects\\_f.lis](#) flat=flat\_av\_norm.fit ccdtype=object  
overca=no trim=no zerocor=no darkcor=n flatcor=yes illumco=no fringed=no readcor=no  
scancor=no fixpix=no biassec=[0:0,0:0] trimsec=[x1:x2,y1:y2]

The trimsection is the same as before. Type “bye” to exit the package.

## 1.6 Extraction of the Source Spectrum

IRAF is capable of performing spectrum and background extraction with the task called “apall”

1. Load the following package twodspec>apextract
2. Check the value of the axis parameter in apextract is set to:
  - 1 for horizontal
  - 2 for vertical slits

epar apextract

dispaxi should be 1 or 2. For WHT it is 2.

### 3. Modifying parameters in apall:

apall [input=@objects f.lis](#) [output=@objects x.lis](#) resize=no extras=no lowers=-6 upper=6  
b\_sample=-50:-20,20:50 b\_naver=-100 b\_niter=1 width=10 nfind=1 maxsep=1000 t\_order=3  
backgro=fit weights=variance clean=yes readnois=5.95 gain=0.989

Here it is important to estimate the background level at each side of the spectrum and this is done by giving two values to IRAF, one of the background region on the left and one on the right. Then IRAF will estimate the average of them and take this value.

b\_sample: specifies the location of the background regions relative to the center of the spectrum.

b\_funct: decides what fitting function it will use(Chevysheb, spline)

b\_otred: specifies the order of the fit

The function “apall” will run and the interactive IRAF aperture environment will appear depicting a plot of pixels vs flux of the first input of the list. The peaks correspond to the sources in the frame.. The main source is usually the highest peak where the aperture is already set. Apertures can be deleted by placing the cursor on the peak and pressing d. A new aperture can be placed by pointing the cursor and pressing m. The background can be seen by pressing b. Ideally this should be resembling a continuous straight line on the 0 flux lever. q returns back to the main plot. If the plot and the aperture choice seems satisfactory, press q again and the instructions for the rest are reported below the plot. A spectrum is obtained which can either be saved or rejected(if for example the aperture is wrongly placed) Hence, q to the next object.

Background: If the background is contaminated, b\_sample can change it as it specifies the location of the background regions relative to the center of the spectrum (e.g. e\_sample=-50:-20,20:50) or when the “irafterm” window appears, type b and then t and then s where the segment is to begin and end and when finished press q.

## 1.7 Wavelength calibration

The following step is the transformation from a pixel to a wavelength scale, that is, to give physical units to the X axis. This is done using the calibration spectrum, meaning the arc images. A calibration or a comparison spectrum is the spectrum taken from a lamp whose gas content is known. Therefore, the resulting spectrum contains a number of spectra lines whose centers are precisely known. By fitting the wavelength centers of those lines with the position in pixels that they occupy in the extracted spectrum the correspondance between pixels and wavelength(angstroms) can be deducted.

Calibration of the spectra with the “apall” tool :

### 1. Extraction of the arc spectrum.

Apall input=arc0001\_s.fit out=arc0001\_x.fit ref=object0001\_f.fit recen-trace-back-intera-

The parameter ref is the reference data image used to extract the spectrum from the arc image. The process has to be repeated for all the arcs.

It is important to remember that usually each image has two arcs and to be sure that the right arc frames are used.

### 2. Identify the arc lines.

This is done with “identify”:

identify images=arc0001\_x.fit section- "middle line" coordli=linelists\$iheneard.dat functio=cheb order=2 zwidth=200 neterat=2 fwidth=9

From the plot 4 or 5 lines have to be identified. Lines that are well distributed along the spectrum pointing them with the cursor and pressing m and interting the actual value which is known from a provided atlas of the lamp. The lamp used for the WHT in the blue part of the spectrum was CuNe and CuAr, 180 sec, and for the red part also one with the same elements but at different part of the spectrum.

A preliminary fit is taken by typing f. What "identify" does is simply create a fitting function that resembles the non-linear behaviour, meaning that, if there was a 1 to 1 correlation between the pixel scale and the wavelength scale then the fitting function would be a straight line. Instead, the arc is like "stretched". The fitting function can be viewed by typing l or the residuals by typing j. With q it returns back to the previous panel. From that point by typing l, "identify" will recognise, according to the fitting function, a number of the strongest lines up to the value given in the parameter maxfeat.

If the selection of these lines is not satisfactory enough for the fitting then the wrong lines can be deleted by typing d whereas new lines can be marked by typing m.

With f a new fit is obtained and the very deviant points are deleted. With q(back or quit) and f(forth) the fit can be changed and the optimal is when the RMS is below 0.5.

To get a value as closer as it can to 0.5 it can be done by pressing f and deleting the values that are located further away from the horizontal line. Then q and f to check the change.

Import notes: it is easier to identify deviant points in the function fitting page and delete the points by pointing them with the cursor and pressing d and this whole process needs to be done only for one image. With q it exits and saves the appertures in the database.

The rest is easy after the arc lines are identified in the first image. With the task reidentify, the first image is used as a reference so as to identify the arc lines in the new image. Attention, if different lamps were used, different wavelenght calibrations should be done to each of them.

For reidentify the command line is :

```
>reidentify images=arc0001_x.fit section- "middle line" nlost=5 coordli=linelists$iheneard.dat interact=no overbose+
```

The assignment od the dispersion solution to the object exposure is done by the tool "hedit" :

```
hedit object0001_x.fits REFSPEC1 arc0001_x.fit add+ ver- show+
```

```
hedit object0001_x.fits REFSPEC2 arc0002_x.fit add+ ver- show+
```

The spectrum source has to know which dispersion solution (relationship between pixel and angstroms) applies. Hedit adds the keyword REFSPEC1 to the header. The content of this keyword is the dispersion solution obtained in the previous step. If there is only one dispersion solution the REFSPEC2 can be ignored.

The dispersion solution can be applied with the help of "dispcor" of IRAF.

```
>dispcor input=@objects_x.lis output=@objects_a.lis lineari=yes global=no samedisp=yes ignoreaps=yes flux=no
```

Once the wavelength calibration is completed, the resulting plot can be examined with splot.

## Identifying Spectra Lines

After obtaining the spectrum of the stars as described above the next step is to identify which lines are shown.

This will be done through iraf's splot which it can normalise the data by itself.

To do this the command is splot and the name of the image:

--> splot

List of images to plot : igr01363\_b\_1\_a.fits

And then an interactive environment will appear on the screen.

The data spectrum appears complicated and with a lot of noise.

By pressing "s" meaning smooth to the window it will clean the spectrum from the noise by taking the mean of the pixels. We choose an even number now 5.

Then the next step is to normalise the spectrum. Since not the whole spectrum has the same mean value we choose to do that by separating it into two. To normalise the spectrum in the interactive environment we press "t" and then "/" .

To cut it into pieces we press "s" and "s" to the area we want to select. We save the normalised spectrum by pressing "i" and write the new name (imagenam\_e\_a.fits) . To continue with the second area (\_b)we repeat the same steps for the rest of the spectrum. The new saved spectra will have the whole spectra saved not just the normalised areas. We will turn the .fits files to ASCII in order to analyse them. In the ASCII files we delete the parts we do not want from the spectra and then load parts a and b to xmgrace.

In order to identify the spectra a given atlas [6] is used that contains classified spectra of identified stars and we compare the spectra lines.

## **7.References:**

- [1] Rivinius, T., Carciofi, A. C., & Martayan, C. 2013, *A&ARv*, 21, 69
- [2] Reig, P., Nersesian, A., Zezas, A., Gkouvelis, L., & Coe, M. J. 2016, *A&A*, 590,A122
- [3] Carciofi , the circumstellar disks of be stars
- [4] Willmarth D., & Barnes J., (1994) *A User's Guide to Reducing Echelle Spectra With IRAF*
- [5] Matthews M., Outmani S., (2018) *A guide for reduction of stellar spectra with IRAF for Skinakas Observatory*
- [6] Walborn, N. R., & Fitzpatrick, E. L. *OB spectral atlas* (1990),*PASP*,102, 379
- [7]Pecaut & Mamajek (2013), *ApJS*, 208, 9
- [8]Steele I. A., Negueruela I., Clark J. S., 1999, *A&AS*, 137, 147
- [9]Simón-Díaz, S., & Herrero, A. (2007). *Fourier method of determining the rotational velocities in OB stars . Astronomy & Astrophysics*, 468(3), 1063–1073.
- [10] Hubeny, I., Lanz T.(2017) ,*A brief introductory guide to TLUSTY and SYNSPEC*
- [11] Skinakas Observatory(2019), *X-ray Binaries*, Retrieved from [http://skinakas.physics.uoc.gr/en/research/xray\\_binaries.html](http://skinakas.physics.uoc.gr/en/research/xray_binaries.html)
- [12] Carroll, Bradley W., and Dale A. Ostlie. *An Introduction to Modern Astrophysics*. Pearson Addison Wesley, 2007
- [13] Varvoglis H., Seiradakis, J.H., *Introduction to modern Astronomy*, Gartaganis Publications, 1994
- [14]Reig, P. (2007) *On the neutron star-disc interaction in Be/X-ray binaries*, *Mon. Not. R. Astron. Soc.*
- [15]Podsiadlowski, Ph., Morris, T., and Ivanova N. 2006, in *Stars with the B[e] phe-nomenon*, ed. M. Kraus, & A. S. Miroshnichenko (ASP, San Francisco), *ASP Conf.Ser.*,355, p. 259.
- [16] Karino, S. (2014). *Bimodality of wind-fed accretion in high-mass X-ray binaries. Publications of the Astronomical Society of Japan*, 66(2), 34.
- [17]Hubeny, I. (1988). *A computer program for calculating non-LTE model stellar atmospheres. Computer Physics Communications*, 52(1), 103–132.
- [18]Hanuschic, R. (1989). *Stellar vsini and optical emission line widths in Be stars. Astrophysics and Space Science*, 161, 61-73.
- [19]Frank J., King A. and Raine D., *Accretion Power in Astrophysics*. Cambridge Astrophysics Series, 1992
- [20] Townsend R. H. D., Owocki S. P, & Howarth I. D., *Be-star rotation: how close to critical?* *Astronomical Society*, 350, 189-195(2004)
- [21] Reig P., Nersesian A., Zezas A., Gkoyvelis L. &Coe M. J. *Long-term optical variability of high-mass X-ray binaries.II. Spectroscopy Astronomy and Astrophysics*, (2016)
- [22] Reig P. & Fabregat, J. *Long-term optical variability of high-mass X-ray binaries.I Photometry Astronomy and Astrophysics*(2015)
- [23] Negueruela I. *On the nature of Be/Xray binaries*, 338, 505–510, *A&A*(1998)